

Electronic Thesis and Dissertation Repository

---

4-7-2022 9:30 AM

## Co-gasification of biomass and plastic waste in a bubbling fluidized bed reactor

Islam ElGhamrawy, *The University of Western Ontario*

Supervisor: Franco Berruti, *The University of Western Ontario*

: Naomi Klinghoffer, *The University of Western Ontario*

A thesis submitted in partial fulfillment of the requirements for the Master of Engineering Science degree in Chemical and Biochemical Engineering

© Islam ElGhamrawy 2022

Follow this and additional works at: <https://ir.lib.uwo.ca/etd>

 Part of the [Other Chemical Engineering Commons](#)

---

### Recommended Citation

ElGhamrawy, Islam, "Co-gasification of biomass and plastic waste in a bubbling fluidized bed reactor" (2022). *Electronic Thesis and Dissertation Repository*. 8527.  
<https://ir.lib.uwo.ca/etd/8527>

This Dissertation/Thesis is brought to you for free and open access by Scholarship@Western. It has been accepted for inclusion in Electronic Thesis and Dissertation Repository by an authorized administrator of Scholarship@Western. For more information, please contact [wlsadmin@uwo.ca](mailto:wlsadmin@uwo.ca).

## ABSTRACT

Plastics are versatile, durable, and can be manipulated to match different needs. The COVID-19 pandemic has demonstrated the importance of reducing plastic waste and is believed to be responsible for increasing the generation of plastic waste by 54,000 tons/day which was reported in 2020. Another widely available waste is biomass waste. Agriculture and agroforestry, forest and wood processing, municipal waste, and the food industry are all considered major producers of biowaste. Co-gasification is considered one of the most promising methods of chemical recycling that targets the production of syngas (hydrogen and carbon monoxide) and light hydrocarbon gases. In this study, the gasification of pure birch sawdust wood (BSD) and pure rice husk (RH) was compared with mixtures where each BSD and RH was mixed with both LDPE and HDPE in the presence of three different bed materials, namely silica sand, olivine, and red mud. It was found that mixing the biomass with LDPE and HDPE increased hydrogen gas ( $H_2$ ) production. The Hydrogen gas concentration in the product gas increased slightly from 10% to 12% by volume when birch sawdust (BSD) was mixed with LDPE with a ratio of 1:1, while the hydrogen gas concentration increased to 15-16% by volume when birch sawdust was mixed with HDPE with a ratio of 1:1 and olivine has been used as bed material. The lower heating value of the produced gas, which has a direct relationship with the hydrogen and light hydrocarbons concentration, increased from 2.8 to 5.7 MJ/Nm<sup>3</sup>. Red mud increased the lower heating value of the produced gas when rice husk was premixed with HDPE from 3-4 MJ/Nm<sup>3</sup> to 5.5-6 MJ/J/Nm<sup>3</sup>, however, the main drawback of using red mud as a bed material was the occurrence of attrition which requires a precautionary measure to control the dust produced and prevent air pollution. The produced gases from the gasification processes are commonly used in internal combustion engines applications, but due to the high

content of hydrogen gas ( $H_2/CO$  range 2-3) in the product, it can be considered a renewable source of hydrogen by further processing the gas mixture to obtain pure hydrogen gas that is utilized in various chemical industries.

**Keywords:** Air gasification, Bubbling fluidized bed, Olivine, Biomass, LDPE, HDPE

## **Abstract for lay audience**

Plastics are widely used all over the globe. The disposed quantities of plastics are increasing daily, as well as agricultural waste. Plastic recycling is challenging and needs an innovative way to keep the environment safe while regaining the value out of that used plastics. Currently, only 10% of the plastic is being recycled with a limited number of turns. Chemical recycling of plastics can recover the material and convert the waste into a valuable material. A technique called gasification is capable of converting plastics into syn-gas ( $H_2$ ,  $CO$ ). The plan is to test a reactor to undergo this process, then mix the plastics with agricultural waste to prevent the plastics from sticking to the reactor. The final stage was studying the effect of different materials (sand, olivine, and red mud) on the syn-gas production when they present inside the reactor at the same time with the plastics. Upon proving the feasibility of this study and overcoming the challenges, It should be possible to scale the reactor to convert more plastics and agricultural waste, preventing the contamination of the environment and providing syn-gas to communities to produce electricity or feeding the syn-gas into the chemical industry.

## **Acknowledgments**

I would like to thank Prof. Franco Berruti and Dr. Naomi for the opportunity to working at ICFAR. They have provided valuable guidance and support throughout my thesis. I would like to acknowledge Dr. Kang for his continuous fruitful guidance and support.

Also, many thanks to Tahereh Sarchami and Thomas Johnston for their highly skilled analytical lab and technical support, respectively.

Finally, I also would like to thank my wife (Nourwanda Serour), my son (Yussuf ElGhamrawy), my father, my mother, and my in-laws for their support and prayers before and during the course of this study.

## **STATEMENT OF CO-AUTHORSHIP**

Islam ElGhamrawy performed all the preparation of the equipment and the gasification experiments.

The major welding has been done by the Western University workshop team. Tahereh Sarchami helped with the analytical work. Franco Berruti supervised the research work.

## Table of Contents

Abstract.....	I
Abstract for lay audience .....	III
Acknowledgments.....	IV
Statement of co-authorship.....	V
1. Introduction and Background .....	1
1.1 Research Motivation .....	1
1.2 Literature Review.....	2
1.2.1 Biomass waste.....	2
1.2.2 Plastic waste.....	3
1.2.3 Waste-to-Resource.....	4
1.3 Gasification .....	6
1.3.1 Gasification reactions.....	8
1.3.2 Gasification temperature.....	10
1.3.3 Equivalence ratio (ER).....	11
1.3.4 Co-gasification.....	12
1.4 Fluidization.....	14
1.4.1 Bed material .....	16
1.5 Tar .....	18
1.5.1 Gas cleaning.....	19

1.5.2	Catalytic treatment .....	20
1.6	Knowledge gap and objectives.....	23
2.	Equipment, material, and methods.....	24
2.1	Bubble fluidized bed gasifier .....	24
2.1.1	Experimental Setup.....	24
2.1.2	Experimental procedures .....	26
2.2	Feedstock (biomass and plastics).....	28
2.2.1	Preparation .....	28
2.2.2	Characterization of the feedstock (biomass and plastics).....	29
2.3	Bed Material.....	31
2.3.1	Preparation .....	31
2.3.2	Characterization of bed materials .....	32
2.4	Experimental plan and methods .....	33
2.4.1	Experimental plan.....	33
2.4.2	Calculating the calorific value HHV/LHV .....	34
2.4.3	Gas yield .....	35
3.	Results and discussion .....	36
3.1	Gasification of pure biomass.....	36
3.1.1	Gasification of pure birch sawdust (temperature variation) .....	36
3.1.2	Gasification of pure rice husk (temperature variation).....	38

3.2	Co-gasification of LDPE pre-mixed with birch sawdust .....	41
3.3	Effect of various bed materials on co-gasification of plastics and biomass.....	43
3.3.1	Effect of olivine as a bed material on co-gasification of plastics and biomass .....	43
3.3.2	Effect of red mud as a bed material on co-gasification of plastics and biomass ....	47
4.	Conclusions, novelty statement, and recommendations .....	51
4.1	Conclusions and novelty .....	51
4.2	Recommendations for further investigation and equipment upgrading .....	52
4.2.1	Feedstock .....	52
4.2.2	Olivine.....	52
4.2.3	Red mud .....	52
4.2.4	Particulate .....	53
4.2.5	Tar.....	53
	Reference .....	54
5.	Appendices.....	64
	Appendix A. Equipment modification.....	64
	Appendix B. Tar accumulation downstream the reactor .....	67
	Appendix C. Air Preheater performance .....	67
	Appendix D. Feeding calibration.....	68
	Appendix E. Order and compositions of feedstock used in different runs .....	70
	Appendix F. Permission for the Table 1-3 and the Figure 1-4 .....	71



## List of tables

Table 1-1 Different conversion technologies.....	6
Table 1-2 Main chemical reactions in the gasification. ....	9
Table 1-3 Blend co-gasification, reprinted by permission from Elsevier .....	13
Table 1-4 Product gas specs requirement for some applications.....	19
Table 2-1 Proximate and ultimate analysis.....	30
Table 2-2 Bed material specifications.....	32
Table 2-3 Chemical composition of Olivine.....	32
Table 2-4 factors and levels used in design of experiments .....	34
Table 2-5 The standard heating values of H <sub>2</sub> , CO, and CH <sub>4</sub> .....	35
Table 3-1 Effect of Temperature on gas composition from pure BSD.....	37
Table 3-2 Rice husk (variation of Temperature).....	38
Table 3-3 Effect of LDPE ratio premixed with birch sawdust as feedstock.....	41
Table 3-4 Examples of agglomerate's structure from rice husk.....	47
Table 3-5 Gasification conditions and gas composition from literature.....	50

## List of figures

Figure 1-1 Global plastic production 1950-2020. Reprinted from statista.com .....	4
Figure 1-2 Gasification categories .....	7
Figure 1-3 Gasification process phases.....	8
Figure 1-4 The relation between gasification temperature and air coefficient .....	11
Figure 1-5 Fluidized bed fluidization regimes.....	15
Figure 1-6 Geldard classification of the powder.....	17
Figure 1-7 Gas cleaning methods classification .....	20
Figure 1-8 Different types of catalysts used to decompose tar compounds .....	21
Figure 2-1 Bubbling fluidized bed reactor scheme including the auxiliary equipments .....	25
Figure 2-2 Porous discs (SS 316L) at the wind box .....	27
Figure 2-3 K-Tron control module .....	27
Figure 2-4 Birch sawdust mixed with LDPE (a-before mixing b-fully dispersed before being fed into the reactor hopper) .....	28
Figure 3-1 Different batches of biomass-plastic mix at ratio 50% .....	43
Figure 3-2 Product gas (dry) components concentration using silica and olivine .....	45
Figure 3-3 Product gas (dry) components concentration using silica and olivine .....	45
Figure 3-4 Ash agglomeration in sand beds a-BSD+LDPE b-RH-LDPE .....	47
Figure 3-5 Red mud feedstock combinations (50%biomass-50%plastic) .....	48
Figure 3-6 Product gas (dry) components concentration using red mud .....	49
Figure 5-1 Blockage of feeding line caused by materials residue. ....	64
Figure 5-2 New manufactured inlet to blow any residue.....	65
Figure 5-3 a- un-sealed hopper b- sealed hopper cap and mounted with valve.....	66

Figure 5-4 Tar accumulated in the reactor-cyclone connection.....	67
Figure 5-5 Screw feeder (uncovered) .....	69
Figure 5-6 Feeding system module throughput at different set points .....	69
Figure 5-7 Calibration the feeding module for Rice husk .....	69

## Nomenclature

**$\varepsilon$** : void fraction

**$\mu$** : viscosity of the fluid

**$\mu\text{g}/\text{m}^3$** : microgram per cubic meter

**$\phi$** : shape factor (sphericity)

**5CB**: CP-Sil 5 CB micro-GC column contains 100% dimethylpolysiloxane

**$d_p$** : mean particle diameter

**$\text{kg}/\text{m}^3$** : kilogram per cubic meter

**kW**: kilo watt

**$\text{mg}/\text{m}^3$** : milligram / cubic meter

**MMT**: million metric tons

**MS5A**: CP-molecular sieve column for permanent gases

**MW**: Mega watt

**nm**: nanometer

**PM<sub>2.5</sub>**: particulate matter 2.5 micrometer

**ppm**: parts per million

**PPU**: PoraPLOT U micro-GC column for halogenated compounds

**$u_0$** : superficial velocity, m/s

## List of Abbreviations

**AAEM**: Alkali and alkaline earth metals

**BFB**: bubbling fluidized bed

**BSD**: Birch sawdust

**ER**: Equivalence ratio

**HDPE**: High-density polyethylene

**HHV**: High heating value

**LDPE**: Low-density polyethylene

**LHV**: Low heating value

**MSW**: Municipal solid waste

**RH**: rice husk

**UN**: United Nations

**VFA**: Volatile Fatty Acid

**WWI**: First World War

**WWII**: Second World War

**XRF**: X-ray fluorescence



# **1. Introduction and Background**

## **1.1 Research Motivation**

UN Sustainable Development Goals were declared back in 2019 to secure a more sustainable globe. Goal number 7 (SDG7), which is considered affordable and clean energy, needs to be addressed as soon as possible to lessen the danger of using high carbon emitter fuels such as coal that was used to produce 42 terawatt-hr in 2019, which represents 25% of the global energy [1]. Goals number 15 and 16, life below water and life on land, suggest giving special attention to our ecosystem. On the grounds of having an increasing supply of plastic waste, as one of the major challenges facing the globe due to its persistence against decomposition and the increasing amount being disposed to the landfills and the oceans (estimated to be 1.6 million tonnes/day [2]), the three pillars of resources recovery should be considered. This study is implementing chemical recycling as an approach to utilize plastic wastes (LDPE, HDPE) efficiently and environmentally friendly by using it as a feedstock that is premixed with another biomass waste and being fed together into a bubble fluidized bed gasifier.

Unintentionally 10-20 million tons of waste plastics reside in oceans [3] when the widely agreed way of disposal is the landfills where plastic may remain in its state for decades without decomposition. There is a huge interest in the recycling of plastics by all stakeholders of the industry. In May 2021, three giant players Dow, LyondellBasell, and NOVA Chemicals announced, “the closed-loop circular plastic fund”, which is \$25 million that is directed to establishing the recovery and recycling of plastics in the USA and Canada. Al Salem et al [5] categorized plastic waste management into four different ways namely primary, mechanical recycling (secondary), chemical (tertiary), and energy recovery.

Rice is being served as a daily meal and is suitable for growing in different countries like China, India, Thailand, and Egypt. Rice husk is the coating of the rice grain and represents around 22% of the total product with an approximate 167.1 million tonnes of RH annually [6]. In many countries, the farmers used to put the husk on fire in the fields because of their low monetary value, which leads to a huge pollution problem due to the smog that is produced [7], [8]. No doubt that the workers in this field are the most affected population due to long durations of exposure to the dust leading to a long list of respiratory problems like phlegm, dyspnea, chest tightness, cough, and nose irritation [9][10]. In addition to the health complications, the CO<sub>2</sub> and CO emissions of the rice husk firing contribute to global warming [11,12].

## **1.2 Literature Review**

### **1.2.1 Biomass waste**

Biomass waste is a common term that is used to describe wastes that are produced from biological activity or biological sources, such as agricultural waste, forestry residue, livestock manure, timber industry waste and a considerable portion of municipal waste [11]. It's not uncommon to have mixed streams of wastes that need to be co-processed especially since the separation of them will impose cost overburden.

Lignocellulosic biomass is the most abundant source of biofuel. The understanding of the characteristics of biomass is essential to understanding and manipulating its behavior during processing [12]. The most significant properties of the reaction include particle size, proximate analysis properties, elemental composition, energy content, and chemical composition. Other properties are more essential from the operational point of view such as grind-ability, density, flowability, moisture sorption, and thermal properties.

Rice is considered as the second most abundant crop waste energy reserve at estimated energy in the range between 3.29 to 15.2 EJ [13]. Rice residue is the inedible fibrous material left in the field after harvesting the rice crop. Farmers in many countries just burn the rice residue and mix its ash with the soil as a fertility source. That process creates a lot of smoke, particulates, and greenhouse gases which exposes the health of the population to hazards and drops the air quality over a wide area (miles away) from the rice fields. The particulate  $PM_{2.5}$  specifically was found to be 44-168  $mg/m^3$  [14] exceeding the US environmental protection agency (EPA) recommendation which is 15, 35  $\mu g/m^3$  yearly average and daily average respectively [15].

### 1.2.2 **Plastic waste**

The COVID-19 pandemic has demonstrated, the indispensable need for plastic products. Plastics are deemed to be versatile, durable, and can acquire proper strength to match different applications' needs. Plastic can acquire a wide range of mechanical, electrical, and optical properties. It is used in almost every application in our daily life such as packaging, electronics, transportation, and sports. Both sectors, the social sector (such as educational premises, shopping stores, governmental premises, etc) and the medical sector experienced a dramatic surge in plastic usage during taking preventive measures to slow down the spread of the COVID-19 virus. Different firms, where the public is supposed to keep a social distance and proper hygiene, were compelled to use plastic products like stickers, banners, signs, and sanitizer bottles to direct the population and promote hand hygiene [2]. The medical sector has the highest leap in plastic wastes production [16]. It is obvious that the production of plastics products is unceasingly growing. Plastics is a synthetic versatile material that is flexible in gaining different properties. A world without plastic is not feasible. Global plastic production has been on a continuous increase since the 1950s (Figure 1-1).

It has increased more than three folds from 100 MMT in 1989 to 368 MMT in 2019 [17]. In 2020, Europe produced 55 MMT of plastic, however only 10.2 MMT of plastic waste have been collected and sent to recycling facilities [18].

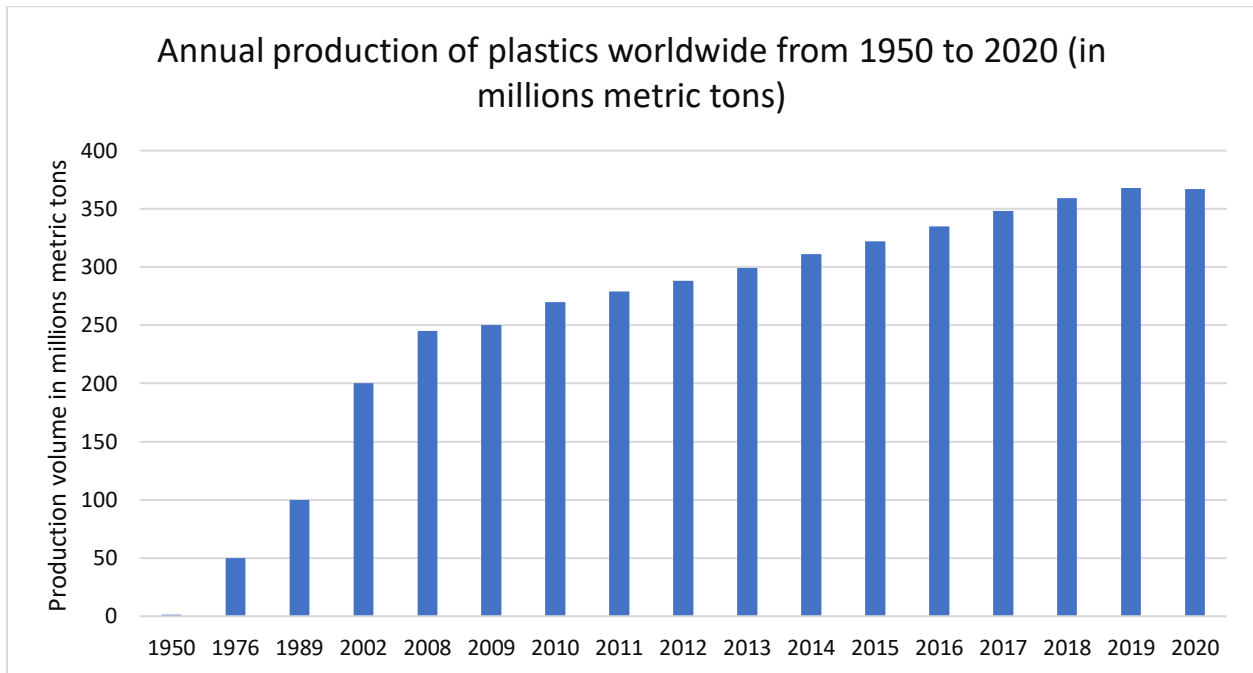


**Figure 1-1 Global plastic production 1950-2020. Reprinted from statista.com [17]**

### 1.2.3 Waste-to-Resource

Plastic waste treatment is predominantly done via three common main processes: Landfilling, mechanical recycling and energy recovery [19]. Landfilling is a major contributor to marine ecotoxicity. Countries strive to generate energy from waste instead of dumping it into landfills due to declining landfill space. Although incineration is considered as an accessible way to recover energy from waste, it is a major source of greenhouse gases emission [20] and toxic compounds would result from incineration [21]. So nations cannot expand more in such technology. Mechanical recycling is mostly accompanied by the degradation of plastic properties limiting the

number of recycling times [22]. Therefore, a more eco-friendly technology needs to be used to recover energy and chemicals out of the waste streams. There are two routes for material conversion which are biological conversion and thermochemical conversion.

The biological conversion includes fermentation and digestion, is usually chosen for non-woody substances that are rich in cellulose that is not highly embedded in a hemicellulose/lignin structure [23]. For example, organic fraction of MSW and waste-activated sludge [24]–[26], and manure [27], [28]. The biological treatment drawback is the long time needed for the microorganisms to consume the feedstock which led researchers to pre-treat the feedstock to shorten the processing period but the pre-treatment is associated with substantial energy consumption, secondary pollution, and additional incurred high cost [29].

Thermochemical processing is a technique that has been proven as an effective way to recover valuable chemicals and energy from complex substances with high efficiencies in low moisture. There are different technologies of thermochemical processing [30][31] such as pyrolysis [32], gasification [33], hydrothermal gasification, hydrothermal liquefaction [34], carbonization (torrefaction), and hydrothermal carbonization[35]. Table 1-1 summarizes the different processing technologies, the water/moisture requirement, and the typical main products.

I have picked up the gasification to tackle this challenge because it yields high quantities of combustible gas which can be utilized to run engines [36], and offers the power to run an electrical generator to produce electricity that can be transported and consumed offsite [37][38], or use the syngas produced to produce fuels and other platform chemicals which are considered of high value [39].

Gas turbines for power generation were originally developed for relatively large-scale plants, but GE Jenbacher gas engines were designed to be suitable for small scale plants. Namely, Jenbacher

J316 gas engine was deployed in Villanova, Torino, Italy to a pyro-gasification of woody biomass in 2011[40] [41]. The paramount advantages of gasification of plastics are the recycling of that liability and production of syngas that can be used in preparing other intermediate chemicals which will be utilized in other products. By this scheme, a zero waste system can be achieved consequently contributing towards a circular economy model.

**Table 1-1 Different conversion technologies**

	Conversion process	Operating temperature °C	Processing time	Drying	Typical main product
Thermochemical conversion	Torrefaction	225-300 °C	hours-days	Needed	charcoal
	Pyrolysis	400-600 °C	minutes - hours	Needed	Bio-oil, biochar
	Gasification	500-1,300 °C	Seconds- minutes	Needed	Syngas
	Liquefaction	300 °C	minutes - hours	Not required	**
Biological conversion	Alcohol fermentation	4-40 °C	1-90 days	Not required	VFA* Biogas
	Anaerobic digestion			Not required	Biogas

\*VFA: Volatile fatty acids

\*\* : products depend on the conditions

### 1.3 Gasification

Gasification is a well-established thermochemical processing technique that was firstly invented by Imbert in the French army during WWI to run vehicles then during WWII. Upon the disruption of the oil supply around the world, it became more demanding to run engines using biomass [42].

It is the thermochemical conversion at high temperature of a carbonaceous feedstock into a

combustible gas (called producer gas or syngas) by using a gasifying agent or agents, such as steam and CO<sub>2</sub> [43]. At the temperature range 600-1,300 °C and a limited amount of oxygen (air gasification), the biomass (hydrocarbon) decomposes into carbonaceous solid, condensable vapours and gases such as hydrogen (H<sub>2</sub>), carbon monoxide (CO) and other gaseous by-products. Gasification can be categorized according to the gasification agent (media): air, steam, and oxygen [33]. Generally, the air is being fed to the gasifier at 20-40% of the stoichiometric quantity (that would be sufficient to complete combustion) to prevent the complete oxidation of the fuel. The gasification process can also be categorized by the interaction mechanism between the gasifying agent and the biomass. The common gasification agents are air, steam, air/steam, and CO<sub>2</sub>. The downdraft is suitable for low to medium capacities 10 kW–1 MW [44], while fluidized bed reactors are suitable for commercial scale-up 110 MW [45] due to efficient heat and mass transfer between the fluids/solids inside the reactor. The fluidized bed will be discussed in depth later in this chapter.

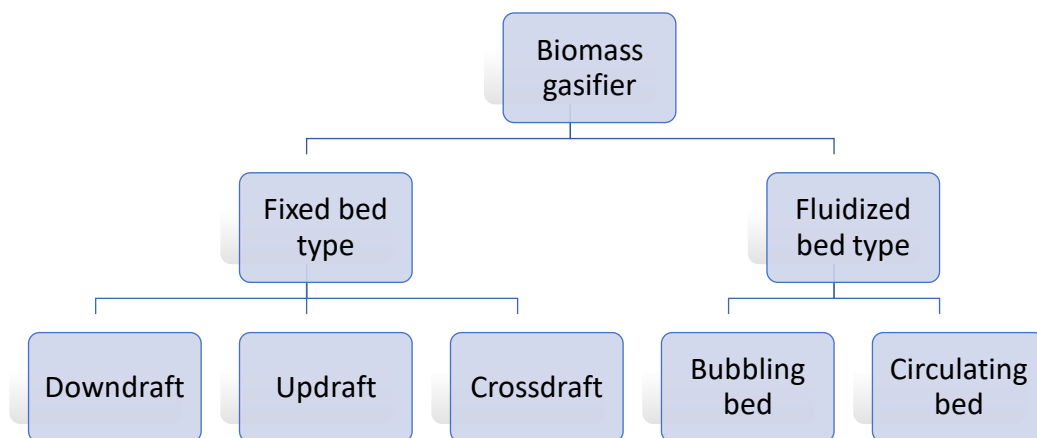


**Figure 1-2 Gasification categories**

A complete gasification process involves four main phases: preprocessing, gasification reaction, gas clean-up and/or reforming, and gas utilization. The first phase is feedstock pre-processing such as size reduction and drying. The second phase is to supply heat to start chemical reactions and enhance using catalysis if applicable. The third phase is the cleaning of the produced gas from the

condensable vapors (mostly tar compounds), reforming the gas into lighter and not condensable hydrocarbons. Finally, the utilization of the product gas in a combined heat and power generation, liquid fuels via Fisher-Tropsch, gas burner, or fuel cell (Figure 1-3).

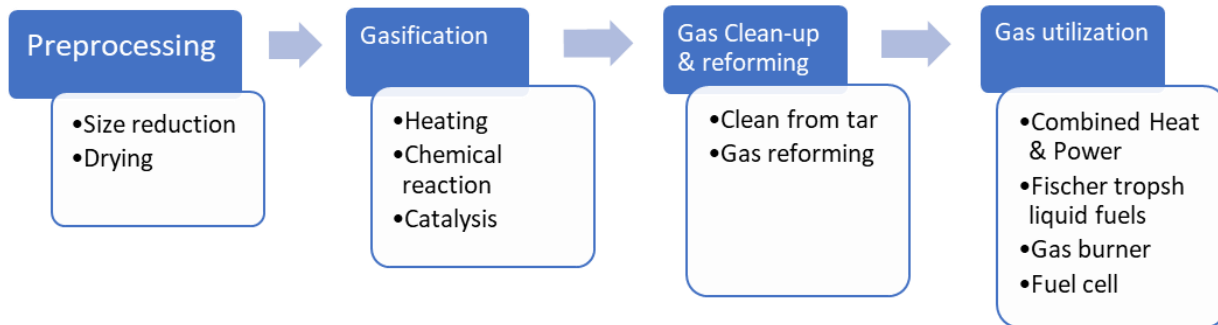
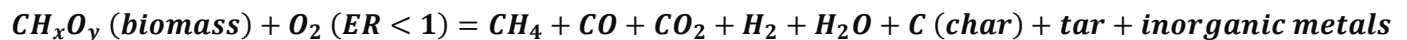


**Figure 1-3 Gasification process phases [46]**

### 1.3.1 Gasification reactions

Gasification takes place at high temperatures employing heating (internally or externally) in the presence of the gasifying agent over a series of reactions of Equation 1-2 to 1-11. The overall reaction can be expressed in Equation 1 as a simplification for typical air gasification. This reaction is an overall reaction that doesn't happen over one step but rather happens through four homogenous and heterogeneous stages [47]–[49]: drying, pyrolysis, oxidation, and reduction (i.e., the gasification reactions).



**Equation 1-1 Biomass overall gasification reaction**

The first stage involves the vaporization of the water content in biomass (moisture) at about 120-200 °C. The second step is the pyrolysis reactions known as devolatilization where light hydrocarbons, tar, CO, and CO<sub>2</sub> are formed. The solids are char and ash. Pyrolysis reactions are endothermic reactions that occur in the temperature range 200-700 °C. The third stage is called

oxidation, or combustion, which entitles the exothermic reactions that lead the temperature to reach 800-1,100 °C, converting the fuel into H<sub>2</sub>O, CO<sub>2</sub>, tar, and hot reactive charcoal. Finally, in the reduction stage, which is a group of endothermic reactions, products from the previous stages react to form the final product gases mainly hydrogen, Carbon monoxide, and methane, the residue is char and ash. Inorganic metals resides in either the char/ash.

**Table 1-2 Main chemical reactions in the gasification adapted from [50]**

Process	Reaction	Specific heating value* MJ/kmol	
<u>Drying</u>	R1 $H_2O_l \rightarrow H_2O_g$		
<u>Oxidation</u>	R2 $C + \frac{1}{2} O_2 \rightarrow CO$	-111	Carbon partial oxidation
	R3 $CO + \frac{1}{2} O_2 \rightarrow CO_2$	-283	Carbon monoxide oxidation
	R4 $C + O_2 \rightarrow CO_2$	-394	Carbon oxidation
	R5 $H_2 + \frac{1}{2} O_2 \rightarrow H_2O$	-242	Hydrogen oxidation
	R6 $C + H_2O \leftrightarrow CO + H_2$	+131	Water-gas
<u>Steam Gasification</u>	R7 $CO + H_2O \leftrightarrow CO_2 + H_2$	-41	Water-gas shift
	R8 $C_nH_m + nH_2O \leftrightarrow nCO + (n + \frac{m}{2})H_2$	Endothermic	Steam reforming
	R9 $CH_4 + H_2O \leftrightarrow CO + 3H_2$	+ 206	Methane Steam reforming
<u>Hydrogen Gasification</u>	R10 $C + 2H_2 \leftrightarrow CH_4$	-75	Hydrogasification
	R11 $CO + 3H_2 \leftrightarrow CH_4 + H_2O$	-227	Methanation
	R12 $C_nH_m + (2n + \frac{m}{2})H_2 \leftrightarrow nCH_4$		Hydrogenation
<u>Carbon dioxide Gasification</u>	R13 $C + CO_2 \leftrightarrow 2CO$	+172	Boudouard
	R14 $C_nH_m + nCO_2 \leftrightarrow 2nCO + \frac{m}{2}H_2$	Endothermic	Dry Reforming

\*Specific heating value is referred at standard conditions (25 °C and 1 atm)

The gasification process is affected by various parameters such as equivalence ratio, reactor temperature, fuel composition, bed material type, and superficial gas velocity. However, the reactor temperature and the equivalence ratio are the most important parameters that affect the heating value of the product gas and its composition [51].

### 1.3.2 Gasification temperature

Gasification temperature has a significant direct relation with the gas yield. According to Le Chatelier's principle, Endothermic reactions tend to shift to the products side at high temperatures. The five main reactions that occur in the gasification process are oxidation, Boudouard, water-gas, methanation, and water-gas shift. These reactions are mentioned in Table 1-2 section 1.3.1 (steam reforming is more significant (dominates) when using steam as a gasifying medium)

Gasification temperature has been repeatedly studied by researchers as it is considered as a main parameter in the process. Emami Taba et al. [52] mentioned in a detailed review paper that  $H_2$ , CO, Carbon conversion, and cold gas efficiency increase as the temperature increases. While  $CO_2$ ,  $CH_4$ , hydrocarbons and tar contents decrease with temperature. That is due to the predomination of endothermic reactions at the temperature. The Hydrogen increases with the rise of the temperature due to the promotion of the endothermic reactions such as R6, R8 and R14 in Table 1-2

The reactor temperature and the temperature profile along the different reactor sections is an important operating parameter for Allo-thermal gasifiers, since the external supply of heat provided to the gasifier can adequately be adjusted to obtain the desired temperature. For autothermal gasifiers, the reactor temperature profile is a state variable of the process, i.e. the system answers to a set of different parameters, such as the equivalence ratio, residence time, chemical energy of the fuel, composition and inlet temperature of the gasifying medium, quality of the reactor insulation, etc. The reactor temperature affects the chemical equilibrium of the main gasification reactions, as can be deduced by the curves in Figure 1-4 An increase from about  $700^\circ C$  to about  $900^\circ C$  leads to an increase in carbon conversion efficiency [53], and gas

yield [54], even though a large amount of residual hydrocarbon products (mainly polyaromatic tars) is generally still detected at this temperature ([55]).

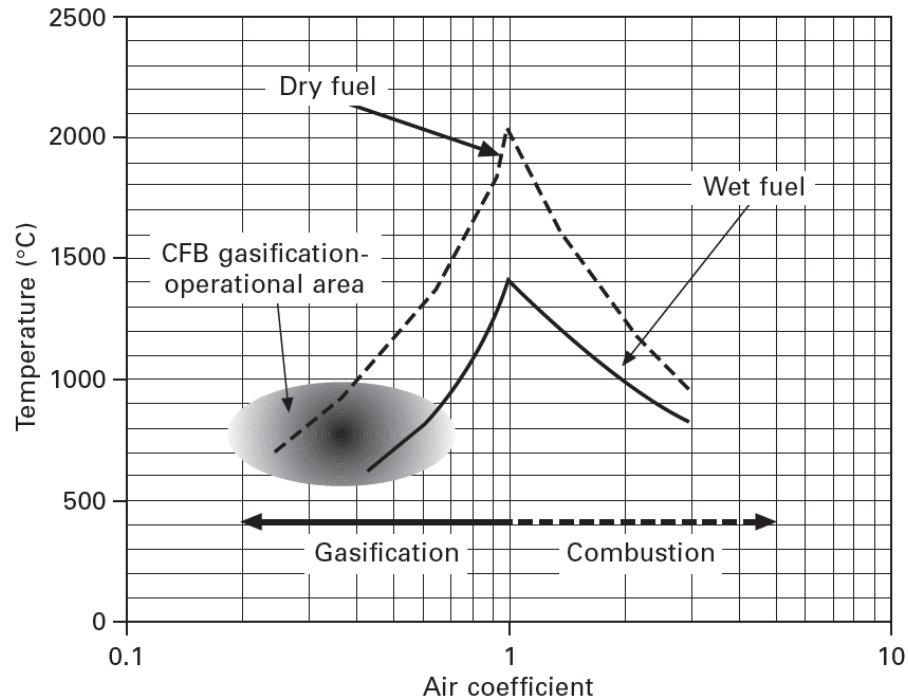


**Figure 1-4 The relation between gasification temperature and air coefficient [56]**

### 1.3.3 Equivalence ratio (ER)

The equivalence ratio is the ratio between the oxygen provided for the reaction to the oxygen that is supposed to be supplied for the complete combustion of the biomass. It has a great impact on the gasifier temperature, producer gas quality, tar content, and gasifier efficiency. The optimum ER has been extensively studied by Park et. al. [57] and Mastellone et al. [58] and many others. They investigated the product gas quality and energy conversion at ER ranges from 20% to 35% then concluded the optimum ratio is around 20%.

$$ER = \frac{\text{Oxygen supplied}}{\text{stoichiometric oxygen required for complete combustion}} * 100$$

### **Equation 1-2**

As the ER increases more than the 20s percent range, the temperature of the producer gas and the quality (H<sub>2</sub> concentration, LHV, ..etc) decrease due to excessive inert nitrogen gas that is introduced to the gasifier [59]. Ma et. al. [60] used rice husk as feedstock and observed that the increase of ER from 17% to 29% resulted in an increase in the gasification reactions, while the tar content reached its lowest value of 1.34 g/Nm<sup>3</sup> at the equivalence ratio of 17-21%. Han et al [61] studied the air gasification of waste plastics in a bubbling fluidized bed stated the highest syngas and methane production were observed was at 15% ER due to the increased oxidation reactions.

#### **1.3.4 Co-gasification**

The gasification of a blend of more than one type of feedstock is called co-gasification. The advantage of co-gasification is the ability to manipulate the composition of the produced gas by varying the feedstock type and the blending ratio, also co-gasification gives the flexibility to accommodate the variation of the different waste streams. The concept of co-processing of different feedstock was implemented in the coal power plant to reduce greenhouse gases and particulate emissions [62]. It has been viewed as a technique to overcome the difficulties faced during the gasification of plastics alone [63] and many combinations showed a positive synergy when processed together at varying ratios [64]. For example, Lopez et al. [65] gasified pure and mixed feedstock of biomass (pinewood waste) and HDPE in a spouted bed reactor in the presence of olivine as bed material. The effect of the co-gasification of HDPE was dramatic in the reduction

of tar and char, where tar from mixed feedstock has been dropped to 16% of the tar produced from pure biomass. Table 1-3 summarizes the benefits of co-gasification of different blends.

**Table 1-3 Blend co-gasification, reprinted by permission from Elsevier (Renewable and Sustainable Energy Review Journal) [66]**

Blend	Advantages of co-gasification	
Biomass-Coal	<p>The addition of biomass in coal gasification reduces the emissions of CO<sub>x</sub>, SO<sub>x</sub>, NO<sub>x</sub>, and H<sub>2</sub>S due to the fewer contents of S, N, and Cl in biomass as compared to coal.</p> <p>Utilization of biomass in coal gasification improves the process reactivity due to the presence of AAEMs (K, Mg, Ca, and Na etc.) in biomass which acts as catalysts during the co-gasification process.</p> <p>The addition of coal in biomass gasification improves the energy density and sustainable availability of feedstock.</p> <p>The use of coal in biomass gasification offers some operational benefits such as less pre-treatment process, ease in the feeding of feedstock, and better fluidization properties that help to reduce the tar content</p>	[49,50]
Biomass-Plastics	<p>The addition of biomass in plastic gasification helps to solve the problem of feeding, lower formation of black powder, and no stickiness problem that are the main issues related to plastic utilization in thermal process.</p> <p>The utilization of plastic in biomass gasification enhances the sustainable usage and disposal of plastic waste for energy production.</p> <p>The addition of plastic improves the energy density of biomass due to higher hydrogen content in plastics and ensure the continued supply of feedstock throughout the year for syngas generation in economical way.</p>	[67][68][69][65]
Biomass-Bio-solids	<p>The co-gasification of biomass/bio-solids have offered the many advantages such as; high volume reduction of bio-solids, reduce pollutant emissions, immobilizing of heavy metals, pathogens, toxic materials, orders, and risks of municipal waste .</p> <p>The high ash content (~35%) of bio-solids can be reduced with the mixing of biomass that mitigates the ash melting problem in gasification process</p> <p>The higher moisture content of bio-solids (70–80%) can be reduced with the addition of dried biomass, which eventually improves the feeding properties of bio-solids .</p>	[70][71] [72][73][74]
Biomass-Petroleum coke	<p>The low reactivity of petroleum coke and high carbon and sulfur emission can be reduced with the addition of biomass, furthermore, AAEMs in biomass ash severs as a natural catalyst in the process.</p> <p>Utilization of petroleum coke offered high energy density due to its high heating value (&gt; 32 MJ/kg), high carbon (&gt; 90 wt%), low ash</p>	[75][76][77]

	content, and low price, which helps to economical commercialization of biomass gasification	
Coal-Black Liquor	The black liquor is a by-product of the pulp and paper industry appeared a prominent source for H <sub>2</sub> production through supercritical gasification with the integration of heat and power . The black liquor usually higher than 80 wt% of moisture content, so its addition can reduce the water consumption for coal-water slurry preparation	[78], [79]
Biomass-Tire	The blend of biomass/tire improves the gasification reactivity, energy density due to the addition of biomass and tire char respectively that solve the disposal issue of polymeric material in environmentally friendly way. It was proven that, the metals in the biomass-char exerted catalytic effect which increased the conversion 5 times compared to tire-char alone.	[68] [80]

#### 1.4 Fluidization

Fluidization is an attractive technique due to the efficient heat and mass transfer that is promoted by good contact between the gases\liquids with the solid bed. It is a widely used process in various industrial processes, such as coal combustion in power plants [81], fluid catalytic cracking in refineries [82], and biomass boilers in pulp and paper mills [83]. Fluidization is a technique that converts a solid bed of particles into a fluid-like material by the means of upward gas that overcomes the downward forces (weight and drag). The acting forces in a fluidized bed are given by the equation below

[weight of solid particles] – [buoyancy acting on particles] = [pressure drop of fluid across the bed] X [bed cross-sectional area]

**Equation 1-3 Forces act on particles during fluidization**

The pressure drop is calculated using the Ergun equation:

$$\frac{\Delta P}{L} = 150 \frac{(1 - \varepsilon)^2}{\varepsilon^3} \frac{\mu u_0}{\phi^2 d_p^2} + 1.75 \frac{1 - \varepsilon}{\varepsilon^3} \frac{\rho_f u_0^2}{\phi d_p}$$

**Equation 1-4 Ergun Equation**

where  $\varepsilon$ ,  $d_p$ ,  $u_0$ ,  $\phi$ , and  $\mu$  are void fraction, mean particle diameter, superficial velocity, shape factor (sphericity), and viscosity of the fluid, respectively.

According to the flow rate of the upward gas the particles bed can assume different states (Figure 1-5). If the flow rate is so low that simply passes through the voids spaces between the particles, the bed is defined as fixed bed.

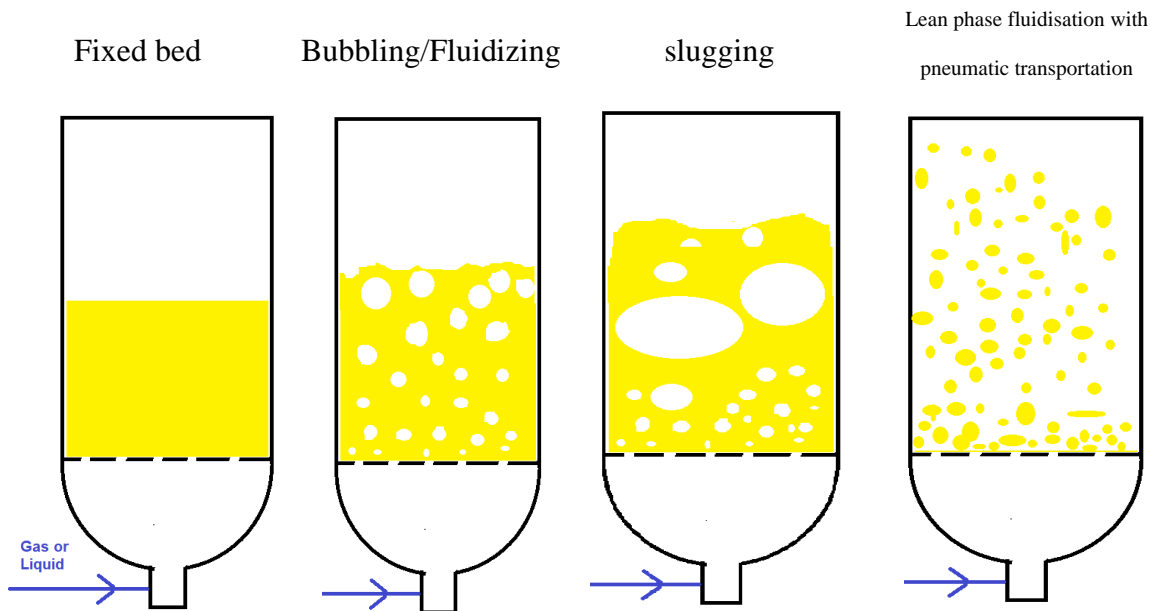


Figure 1-5 Fluidized bed fluidization regimes

With an increase in flow rate where the upward force counterbalances the weight of the particles, the pressure drop through any section of the bed equals the weight of fluid and particles in that

section. This is defined as expanded bed. The velocity at which the bed starts to expand is defined as minimum fluidization velocity (Equation 1-5).

$$U_{mf} = \frac{(\rho_p - \rho_g)^{0.934} g^{0.934} d_p^{1.8}}{1,111 \mu^{0.87} \rho_g^{0.066}}$$

**Equation 1-5 Baeyens' equation for minimum fluidization velocity**

where  $U_{mf}$ ,  $g$ ,  $\rho_g$ ,  $\rho_p$ ,  $d_p$ , and  $\mu$  are the minimum fluidization velocity, gravitational velocity, gas density, particle density, particle diameter, and gas dynamic viscosity respectively.

The minimum fluidization velocity is the minimum superficial velocity that allows the gas to suspend/fluidize the solid particles of the bed. It depends on the same parameters mentioned Equation 1-4. Fine particles exhibit a type of behavior that is not found in the coarse particles, which is the ability to be fluidized at velocities beyond the minimum fluidization velocity.

A good mixing of particles and a uniform heat profile through the bed are achieved when the bed is fluidised. The mixing happens when the bubbles formed by the upward gas reach the surface of the bed. Then, they collapse causing the bed surface disturbance which enhances the heat and mass transfer at the surface of the bed. The bubbles coalesce as they raise through the bed, consequently, the bubble volume increases with distance from distributor. The bubble will either reach its maximum volume before reaching the top of the bed or got constrained with the reactor size. In the second case the bed is called to be slugging. Slugging behaviour results in lower heat and mass transfer.

#### 1.4.1 **Bed material**

Derek Geldard studies different fluidization behaviour of beds over a range of particle sizes. He classified the bed material according to its size and behaviour into four groups namely A, B, C, and D. The fluidization phenomena have been found to be dependant on the density difference

between solid particles and the fluidizing medium, and the mean particle size. Geldart [84] has classified powdered into 4 categories including A, B, C, and D (Figure 1-6).

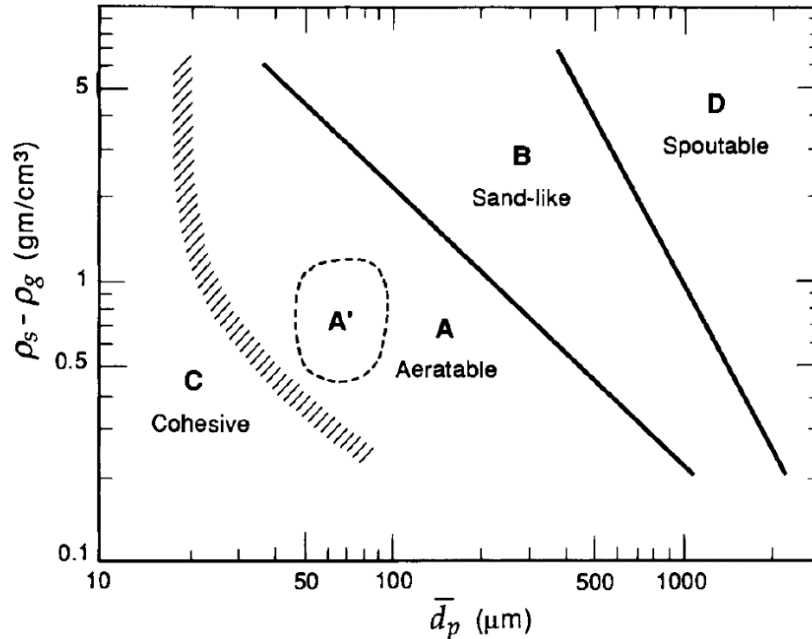


**Figure 1-6 Geldart classification of the powder**

Group A powder resembles a widely used materials in the commercial fluidized bed catalytic reactors where the interparticle forces are present. Group A beds shows a significant expansion at velocities between minimum fluidization velocity and bubble velocity. Bubbles exhibit resistance while flow in the dense phase due to the cohesion effect between the particles. Group B is the one we are interested in its behavior because the absence of the cohesion forces between the particles and the bubbles appear just at the minimum fluidization velocity. It is commonly used for its bubbling regime right upon the minimum fluidization velocity. Bed expansion is small and it collapse once the upward gas shut off. The average particle size of group B ranges from 80-600  $\mu\text{m}$  when the density of the used particles is around 3  $\text{gm}/\text{cm}^3$ . Group C describes the finest powder (like flour, or cement) where no bubbles can form in the bed due to the strong cohesion between the powder particles. Group D describes the large and/or dense particles where they tend to cause

the gas to spout (flow in one channel and mix the particles that are near the channel), so that the gas flows into the base of the bubble and out of the top without propagating more bubbles [84] [85].

In case of fluidization of group B powder, the bed may exhibit different fluidization regimes according to the gas velocity, consequently the forces acting on the particles (Figure 1-5).

## 1.5 Tar

Tar from an operational point of view is an undesirable black sticky hydrocarbon material that is produced when treating the biomass or the plastic in a thermochemical process like pyrolysis or gasification. It is an undesired by-product due to the deposition on downstream lines and equipment (such as piping/generator) or the deposition over the bed material/catalyst inside the reactors. Thus, the operators must optimize the operating parameters to prevent/reduce the tar formation to minimize the shutdown of the operation due to sintered or poisoned bed/catalyst or fouling downstream the reactor. Researchers classified the tar into primary tar, secondary tar, and tertiary tar [86]. Primary tar is produced during the pyrolysis stage of the matter gasification, then undergoes further cracking into secondary and tertiary tar compounds (check section 1.3.1 for gasification stages). At 400 °C range, the tar is mainly the primary product (mixed oxygenates) that crack at a higher temperature into phenolic compounds (phenolic ethers and alkyl phenolics) then as the temperature increases to 700 °C they crack into aromatic hydrocarbons.

### 1.5.1 Gas cleaning

Gas produced from the gasification process must meet certain criteria to achieve trouble-free operation for a continuous period and minimize shut down of the equipment that consumes the product gas. Downstream operations, such as internal combustion engines, gas turbines, fuel cells, Fischer-Tropsch reactor, or methanol synthesis critical requirement is summarized in Table 1-4.

**Table 1-4 Product gas specs requirement for some applications [87]**

Process	Contaminant	Level	Reference
Internal combustion Engine	Tars	< 10 mg/Nm <sup>3</sup>	[88]
Compressors	Tars	50-500	[89]
PEM fuel cells	H <sub>2</sub> S	<1 ppm	[90]
Methanol synthesis	Tars	<0.1 mg/Nm <sup>3</sup>	[87]
	NH <sub>3</sub>	10 ppm	
	HCN	0.01 ppm	
	Total Sulphur	0.5 ppm	

The internal combustion engine has the most tolerable upper intake levels. The tar, as mentioned in part 1.4.2, is an undesirable viscous liquid that condenses at low temperature over the exit lines and inside equipment downstream the gasifier causing an unnecessary shutdown.

Two approaches are considered for cleaning product gas: In-situ tar reduction (primary) or post gasification tar reduction (secondary). The first one targets the minimization of the formation of tar by pre-processing the feedstock or by varying the operating parameters of the gasifier. The latter option is to crack the tar after it has been formed by raising the temperature of tar or have the tar pass over a catalyst post the reactor before it cools down, both are known as thermal and catalytic cracking methods respectively. Hot gas filtration is also a gas cleaning method, its drawback is the continuous pressure drop while deposition of the contaminants filter cake.

Figure 1-7 summarizes the classification of the various approaches.

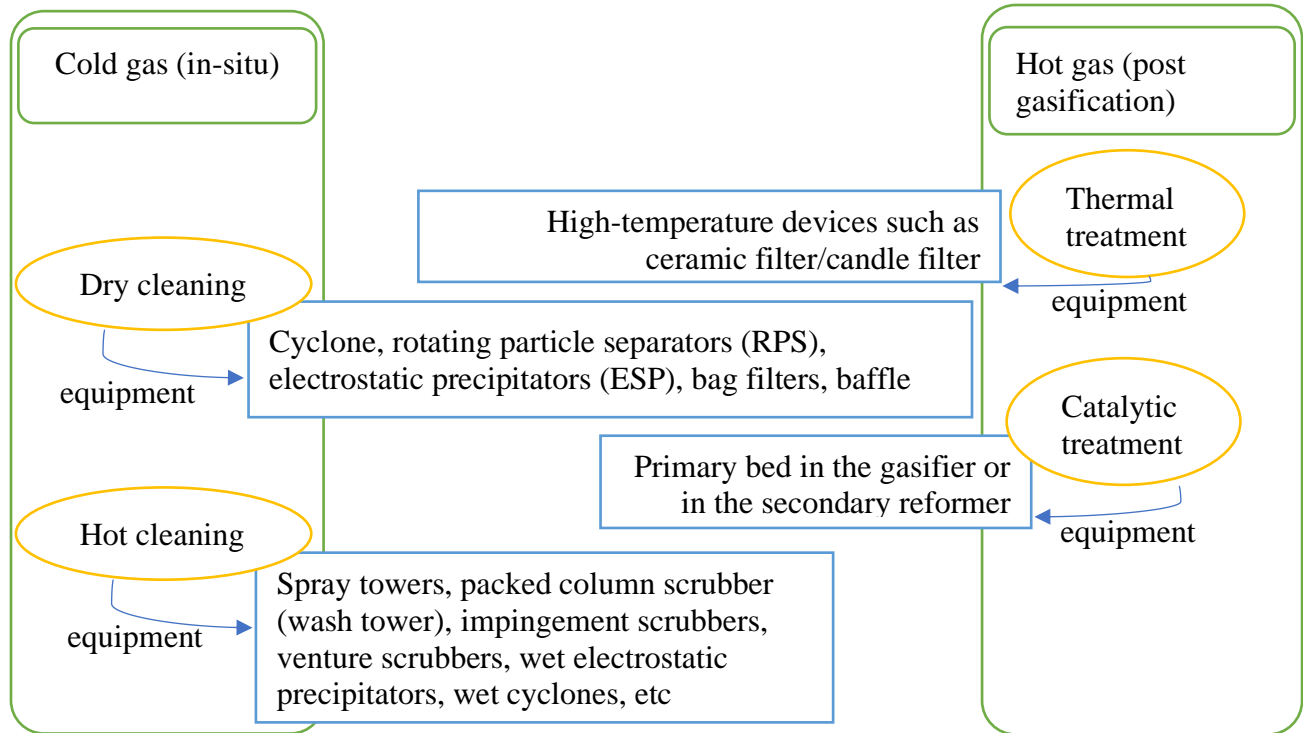


**Figure 1-7 Gas cleaning methods classification**

### 1.5.2 Catalytic treatment

Different types of catalysts have been studied aiming to have the capability to convert the feedstock and the product tar into useful products in the presence of the other main products ( $H_2$ ,  $CO$ ,  $CO_2$ , and  $H_2O$ ) in the temperature range  $600-800\text{ }^\circ\text{C}$  where most gasification processes take place. Resistance to deactivation is another aspect that is usually addressed specifically with biomass that contains high sulphur content. Other objectives are being targeted in the catalyst such as good mechanical strength, cost-effectiveness, and non-toxicity. Walter Torres et. al. [91] have stated many catalysts that have been used in various studies and summarized in Figure 1-8.

Acidic	Basic	Iron based	Nickel based
<ul style="list-style-type: none"> <li>□ acidic zeolites</li> <li>□ silica-alumina</li> <li>□ hetero-poly-acids</li> <li>□ sulfated metal oxides</li> </ul>	<ul style="list-style-type: none"> <li>□ alkaline earth metal oxides</li> <li>□ alkali ion-exchanged</li> <li>□ alkali ion-added zeolites</li> <li>□ clay minerals</li> <li>□ alkali metal ions supported on silica or alumina</li> </ul>	<ul style="list-style-type: none"> <li>□ Sintered Iron</li> <li>□ Ankerite</li> <li>□ Iron pellets</li> </ul>	<ul style="list-style-type: none"> <li>□ Ni-MgO</li> <li>□ Ni-Al<sub>2</sub>O<sub>3</sub></li> </ul>

**Figure 1-8 Different types of catalysts used to decompose tar compounds**

A recent technique has been used by Shen et al. [92] to produce a more sustainable catalyst by mixing Iron (Fe), Nickel (Ni), and biochar produced from slow pyrolysis of rice husk. It has been noticed that heavy tar removal efficiency increased to 42% and 93% when used biochar and Ni-Fe-Char as catalysts respectively.

A fluidized bed catalyst is under movement all the time, which dictates the resistance to attrition to be an important feature in the proposed catalyst. Olivine, which contains high alkali metals (Ca, Mg oxides) is attractive for that purpose [93] [55] [94] [95]. Olivine has been used as a bed material by Serrano et al. [96], the produced gas showed high concentrations of hydrogen. It was proven that the olivine yields high-quality gas and the chemical energy transferred into the gas was 87% of the feedstock (*C. cardunculus* L.). Untreated olivine was used in the gasification of sunflower and willow. The tar reduction has been reported to be approximately 40% less than that produced while using silica along with an increase in the hydrogen yield. The attrition resistance has been

examined for calcined olivine, and un-treated olivine, it has been reported that minimal decrease of attrition resistance was observed on the uncalcined olivine [97].

Red mud, also known as bauxite residue, is a solid waste material generated from the processing of bauxite using the Bayer process to produce alumina. It is considered a promising cheap source of iron-based catalysts. Karimi et al. [98] reduced the red mud then mixed it with pyrolysis bio-oil to increase the stability of the oil. It showed high catalytic activity by suppressing the reactivity of the oxygenated compounds. Red mud mixed with gasification biochar was able to achieve high conversion of naphthalene (tar model component) in a wet syngas environment but the coke deposition was severe which has been controlled by acid activation. The tar conversion was low when used the red mud was without activation. Cheng et al. reported also that the catalytic activity of red mud was dropped significantly in the presence of the steam in steam gasification [99].

## **1.6 Knowledge gap and objectives**

To present the basic gaps for this study, a through literature review was performed to understand the current state of research related to fluidized beds used for gasification of biomass and plastics. Based on the review, and to the best of my knowledge, many researchers exerted efforts in the air co-gasification of biomass with coal but only few of them mixed the biomass with plastics. Moreover, olivine hasn't been intensively studied as a catalyst for air gasification of biomass-plastic mixture. Red mud, which is a major challenge that faces aluminum industry and is considered an iron-based catalyst, hasn't been used in air gasification process as a bed material.

This study is targeting the conversion of both biomass and plastic wastes into a valuable resource by studying the quality of the product gas that is produced from co-gasification of birch sawdust and rice husk when mixed with virgin LDPE and HDPE at high temperatures in a bubbling fluidized bed gasifier. I will investigate the feasibility of conversion of each biomass solely to address the needs of the forestry waste producers as well as the rice crop field owner.

I will assess the practicality of adding plastics at different ratios to the biomass feed to examine the operability of processing mixed feedstock because the real-life wastes can be found mixed.

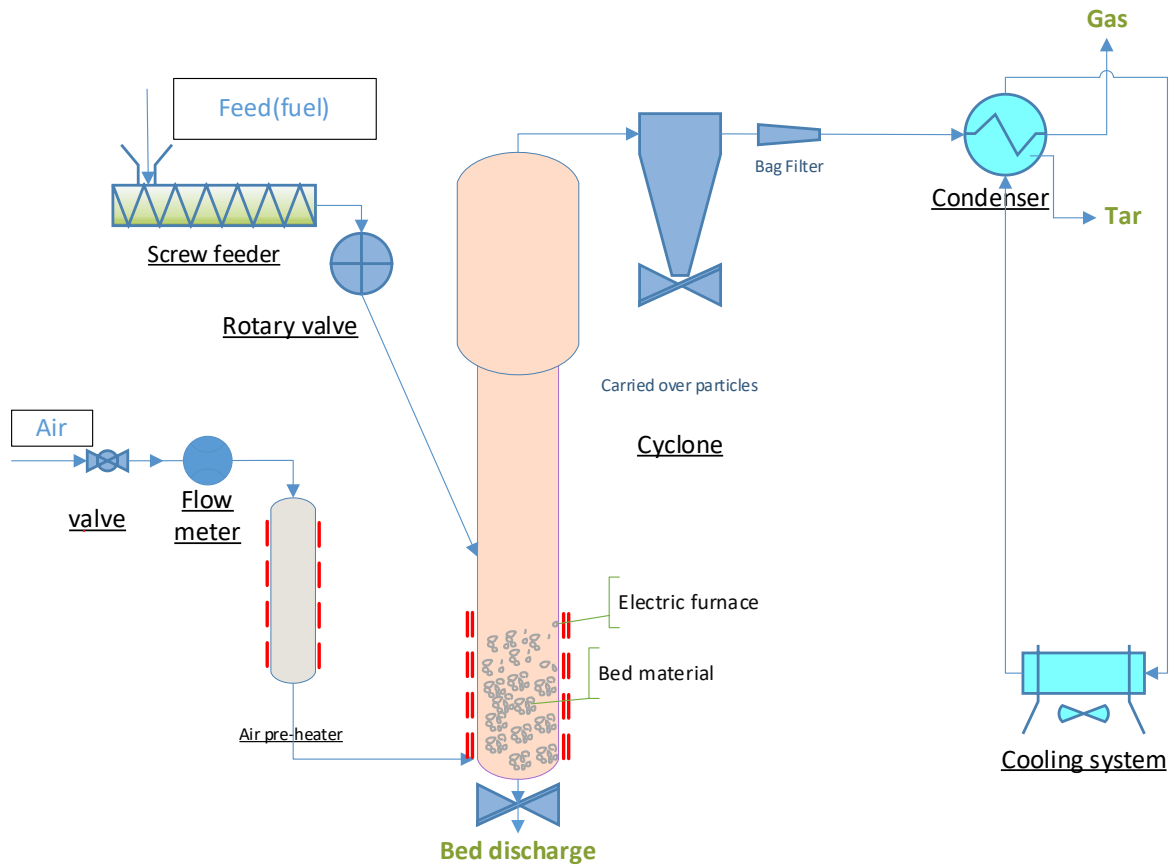
The woody biomass will be mixed with the two types of plastic to investigate the synergy and compare it to the synergy between the rice husk and the same plastic species. In addition to the variation of the premixed feedstock, the variation of the fluidized bed material will be tested. Silica sand has been considered as the control state, Olivine sand, which is a cheap, active material, and Red mud, which is also known as bauxite residue, will be used as a catalytic bed material. This study aims also to assess the process applicability and identifying any challenges in utilizing both materials.

## **2. Equipment, material, and methods**

### **2.1 Bubble fluidized bed gasifier**

#### **2.1.1 Experimental Setup**

The experiments were conducted in a lab scale Bubbling Fluidized Bed Gasifier (BFBG) located at the Institute for Chemicals and Fuels from Alternative Resources (ICFAR). A scheme of the BFBG is shown in Figure 2-1. The reactor is made of stainless steel 316L and its total height is 1.75 m. The inner diameter is 76 mm in the bed area and 100 mm in the freeboard zone. The setup is equipped with two electric furnaces to heat the column and to preheat the fluidization air which is being pumped through 10 porous discs (Figure 2-2), a screw feeding system combined with a rotary airlock valve, a cyclone for removal and collection of small particles in the effluent gas, a bag filter housing, a primary air inlet (the fluidization gas) and a secondary air inlet on the freeboard to assist volatile combustion (the latter was not used in this study), a water-cooled condenser for tar removal, and a product gas sampling port. The non-condensable gases are vented outside. I have done some modifications to the setup to increase the operability and reliability of the reactor, different modifications were made and they are reported in Appendix A.



**Bubbling Fluidized Bed setup**

**Figure 2-1 Bubbling fluidized bed reactor scheme including the auxiliary equipments**

The reactor monitoring and control system consists of 6 thermocouples, 2 pressure transducers and 2 pressure gauges located at different positions in the system. The signals from the thermocouples and the pressure transducers were monitored by a handheld data logger which was later upgraded to an Arduino data acquisition system connected via USB port to an external laptop equipped with a custom-designed code to acquire, record, save the various readings from the thermocouples and the pressure transducers.

### 2.1.2 **Experimental procedures**

A detailed Standard Operating Procedure (SOP) document (separately) was prepared during the maintenance and commissioning stage before commencing the experimental runs. Before each test, approximately 2.5-2.8 kg of bed material were inserted, which corresponds to a static height of 23-26 cm. This height was thought to be optimal for heat transfer from the external furnace to the bed. The feedstock is pre-mixed and added to the feeding hopper which is higher than the feeding port in the reactor. Using a double screw feeder and K-Tron control module (Figure 2-2) the feeding rate is discharged precisely from the screw feeder into the reactor passing through a rotary airlock valve which helps the reduction of back flow of the gases into the feeding system. The feeder was calibrated for each feedstock before the experimental runs (Appendix D) to account for the different biomass size and composition. Both furnaces were switched on to reach the desired temperature of 750-950 °C and kept at that temperature 30 minutes. The total heating process is 90-120 min.

The pre-heated flowrate of air is controlled using a flowmeter and it was adjusted to keep the solids bed under bubbling fluidization state. Its temperature was measured throughout the runs and it was ranging from 190-360 °C, depending on the rate of the air flowing inside the heater. It was noticed for the range 10-20 scfh that as the rate of the air increases the heat transfer improves, consequently the exit temperature of the air increases, and vice versa (Appendix C).

The feedstock was being fed after all temperatures stabilize. Gas samples were collected post the condenser using gas bags.

Collecting the gas from the gas sampling point at the end of the condenser was carried out after 20, 25, and 30 minutes since the start of feeding. 1 L Tedlar<sup>®</sup> gas sampling bags were used to sample the syngas after the condenser. The gas samples were analyzed using a Varian micro GC

CP4900 instrument that is equipped with three columns; 10m MS5A, 10m PPU, and 8m 5CB, while the carrier gases were Helium and Argon.

After collecting the gas and stopping the feed, The furnace was left running for 30 minutes to make sure that the whole feed was processed. The hopper was emptied before introducing any other feedstock type.

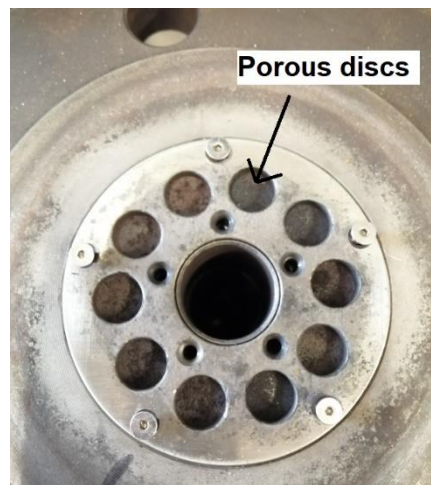


**Figure 2-2 Porous discs (SS 316L) at the wind box**



**Figure 2-3 K-Tron control module**

## 2.2 Feedstock (biomass and plastics)

### 2.2.1 Preparation

Two types of biomass have been used in this study. The birch sawdust used in this study was obtained from ICFAR stock, while the rice husk has been obtained from Texas, US.

Both biomass feed have been ground, sieved, sorted according to its particle size. Only two ranges have been used (0.3-0.85 mm and 0.6-1.4 mm). I used standard test sieves from W.S Tyler to control the particle size range for each run to prevent discrepancies in the feeding rate. The list of sieves included No.14, No.20, No. 30, No. 50 (1.4 mm, 850  $\mu\text{m}$ , 600  $\mu\text{m}$ , 300  $\mu\text{m}$ ).

Both Low-Density Poly Ethylene (LDPE) and High-Density Poly Ethylene (HDPE) were obtained from NOVA Chemicals® in Sarnia, Ontario. LDPE grade is widely used in shrink wrap, food packaging wrap, and dispensing bottles. HDPE is generally used in manufacturing chemical containers (shampoo, detergents...etc), milk jugs, pipes, and automotive parts. The mixtures were premixed rigorously before being fed to the hopper (Figure 2-4).

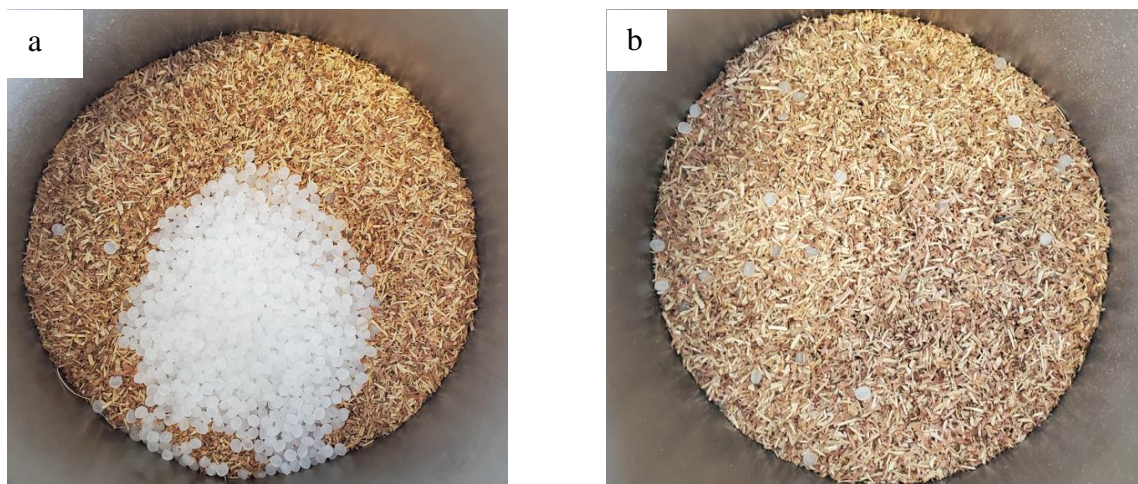


Figure 2-4 Birch sawdust mixed with LDPE (a-before mixing b-fully dispersed before being fed into the reactor hopper)

## 2.2.2 Characterization of the feedstock (biomass and plastics)

### 2.2.2.1 Proximate analysis

The biomass and the plastic have been analyzed by proximate analysis to assess the amount of volatile matter (VM), fixed carbon (FC), and ash content according to the ASTM D1762. First, birch sawdust/ rice husk were ground and sieved to a particle size of 1mm, then dried in the muffle oven at 105 °C for 2 hours to remove the moisture. Then, raise temperature to 950 °C and 750 °C for 6 minutes and 6 hrs to measure volatile matter and ash, respectively. The proximate analysis to be measured after each heating stage.

$$\text{Moisture, \%} = [(A-B) / A] \times 100$$

#### Equation 2-1 Moisture from proximate analysis

where: A = grams of air-dry sample used, and B = grams of sample after drying at 105 °C.

$$\text{Volatile matter, \%} = [(B-C) / B] \times 100$$

#### Equation 2-2 Volatile matter from proximate analysis

where: C = grams of sample after drying at 950 °C

$$\text{Ash, \%} = D/B \times 100$$

#### Equation 2-3 Ash from proximate analysis

Where D = grams of residue

$$\text{Fixed Carbon, \%} = 100 - (\text{Moisture} - \text{Volatile matter} - \text{Ash})$$

#### Equation 2-4 Fixed carbon from proximate analysis

### 2.2.2.2 Ultimate analysis

Ultimate analysis was conducted to determine carbon, hydrogen, nitrogen, and oxygen content, using Thermo Flash EA 1112 elemental analyzer (CHNSO). The system was calibrated using the

first four samples, 0.5, 1, 2, and 2.5 mg of BBOT (2,5-Bis (5-ter-butyl-benzoxazol-2-yl) thiophene) (CE Elantech, NJ, US) [100]. Each of the tin capsules contained 1-2 mg of biomass or plastic and 8-10 mg of vanadium pentoxide to achieve complete conversion of sulphur. Samples were combusted at 900°C in a stream of helium with a known volume of oxygen. This technique produces N<sub>2</sub>, CO<sub>2</sub>, H<sub>2</sub>O, and SO<sub>2</sub>, which were then subjected to separation and quantification using gas chromatography, which comprises a steel column 2 m long and 5 mm in diameter, and helium as a carrier gas (flow rate of 140 mL min<sup>-1</sup>). Finally, the elements were detected using a Propack model thermal conductivity detector (TCD). The oxygen content was determined by difference.

The results of both proximate and ultimate analysis for the fuel studied are reported in Table 2-1.

**Table 2-1 Proximate and ultimate analysis**

Material	Ultimate analysis (wt%, dry basis)					Proximate analysis (wt%, dry basis)				HHV (MJ/kg)
	C	H	O*	N	S	MC	VM	Ash	FC*	
BSD	44.8	5.6	49.5	0.14	0	9.17% ± 1.02%	81.98% ± 0.86%	1.03% ± 0.09%	7.83% ± 0.24%	16.83
RH	37.4	5.5	56.0	1.02	0.08	10.24% ± 0.05%	66.67% ± 0.33%	16.83% ± 0.08%	6.24% ± 0.28%	14.60
LDPE	83.5	12.9	3.1	0.03	0.40	0.02%	99.96% ± 0.06%	-	-	46.56
HDPE	83.6	9.1	1.6	1.53	0.38	0.03%	99.97% ± 0.03%	-	-	46.75

\*: by difference

## **2.3 Bed Material**

### **2.3.1 Preparation**

The first bed material used in this work was silica sand ( $\text{SiO}_2$ ) particles brought from Optaminerals, Ontario, Canada, with a particle density of  $2,860 \text{ kg/m}^3$ . The sand was sieved to a particle size of  $300\text{-}600 \mu\text{m}$  (US mesh No.30 and 50) (resulting in Geldart group B particles).

The second bed material used in this work is olivine sand (magnesium iron silicate,  $(\text{Mg,Fe}_2)\text{SiO}_4$ ) brought from ICFAR in-stock chemicals, with a particle density of  $3,340 \text{ kg/m}^3$ . The olivine was used at a size distribution of  $177\text{-}250 \mu\text{m}$  (US mesh No.80 and 60) (resulting in Geldart group B particles).

The red mud is considered an environmental liability due to being waste from the aluminum industry process, it has been obtained from Alcan International Ltd., Canada as slurry. The water content varies according to the source and time spent in the tailing ponds before being transported. I had to dry the slurry at  $105 \text{ }^\circ\text{C}$  for 12 h before being able to crush it using a mortar. After drying, the red mud was sieved to a particle size of  $177\text{-}250 \mu\text{m}$  (US mesh No.80 and 60) (resulting in Geldart group B particles). Its density was found to be  $2,670 \text{ kg/m}^3$ .

It is part of the experimental procedure to maintain the bed material at the target temperature of the experiment for at least 60 minutes and not more than 90 minutes before commencing the feedstock.

### 2.3.2 Characterization of bed materials

Specific surface area, average diameter, bulk density and pore volume are summarized in

Table 2-2

**Table 2-2 Bed material specifications**

Bed material	BET surface area, m <sup>2</sup> /g	Size range, $\mu\text{m}$	Bulk density, kg/m <sup>3</sup>	Average pore size, nm	Total pore volume, cm <sup>3</sup> /g
Silica sand	-	300-600	2,860	-	-
Olivine sand	2.734	300-600	3,340	3.751	0.0026
Red mud	12.181	177-250	2,670	3.446	0.0209

The chemical composition of olivine can be explored using XRF. A typical composition of olivine is mentioned in Table 2-3 [101]

**Table 2-3 Chemical composition of Olivine**

Compound	Fraction (wt%)
MgO	42.19
SiO <sub>2</sub>	40.97
CaO	7.21
FeO	6.71
Al <sub>2</sub> O <sub>3</sub>	2.84
Cr <sub>2</sub> O <sub>3</sub> +TiO <sub>2</sub> +K <sub>2</sub> O	0.08

Red mud as mentioned earlier is a by-product of alumina processing so the dominant compounds are Fe<sub>2</sub>O<sub>3</sub>, Al<sub>2</sub>O<sub>3</sub>, SiO<sub>2</sub>, TiO<sub>2</sub>, CaO, and Na<sub>2</sub>O [98].

## 2.4 Experimental plan and methods

### 2.4.1 Experimental plan

Both types of biomass have been gasified separately in the reactor in the presence of one of the three bed materials to study the effect of the bed material alone at the same equivalence ratio and temperature. The equivalence ratio, which is the ratio of the air supplied to that needed for complete combustion has significant effect on the fluidization behaviour of the bed. ER was fixed to prevent the hydrodynamics changes from influencing the results. The gasification has been studied at low temperature (750 °C) and high temperature (950 °C) for pure birch sawdust. Another set of experimental runs has been conducted using birch sawdust mixed with LDPE at different concentrations 15%, 30%, 50%wt (LDPE weight/sample weight) to study the effect of increasing LDPE on the product gas quality. For each test using 50% LDPE, another test using 50% HDPE was undergone to compare the LDPE vs the HDPE. The novelty in this work is the examination of the red mud effect on the product gas in comparison with silica sand and olivine sand. List of the experimental parameters is in Table 2-4. Pre-mixing has been done prior feed to the hopper. Precise tuning of biomass flow was not directly corresponding to the feeding module because the module controls the speed of the screw feeder not the mass of the materials being fed. Therefore, I had to calibrate the feeding rate for each biomass, plastic, and their combinations Appendix D. The calculated ER values are based on the air flow rate and the biomass/plastic ultimate analysis are given in Table 2-1.

The temperature of the majority of the runs was 850 °C due to the higher yield of hydrogen noticed during biomass gasification.

**Table 2-4 factors and levels used in design of experiments**

Factors Levels	Temperature (°C)	Feedstock	Bed material
	750	BSD 100%	Silica sand
	800	RH 100%	Olivine sand
	850	BSD+50% LDPE	Red mud
		BSD+50% HDPE	
		RH+50% LDPE	
		RH+50% HDPE	

#### 2.4.2 Calculating the calorific value HHV/LHV

The higher heating value (HHV) and lower heating value (LHV) are commonly used as a measurement for the energy content. HHV is defined as the total amount of heat of material including the latent heat of vaporization of water vapor produced during the combustion of the material. LHV is similar to HHV excluding the latent heat of vaporization of water vapour. Energy consumers are more interested in the LHV whenever it's not practical to recover the heat of vaporization from the combustion product stream. HHV is determined experimentally using bomb calorimeter according to ISO 1928:2020 (Coal and coke- determination of gross calorific value), ISO 18125:2017 (solid biofuels), or by calculation based on ultimate (elemental), proximate and structural (chemical) composition. I have used the bomb calorimeter to measure the HHV of the feedstock. For the product gas calorific value calculation, Equation 2-5 was used. Table 2-5 shows the standard heating values of H<sub>2</sub>, CO, and CH<sub>4</sub> [102].

$$HHV \left( \frac{MJ}{Nm^3} \right) = X_{H_2} * HHV_{H_2} + X_{CO} * HHV_{CO} + X_{CH_4} * HHV_{CH_4}$$

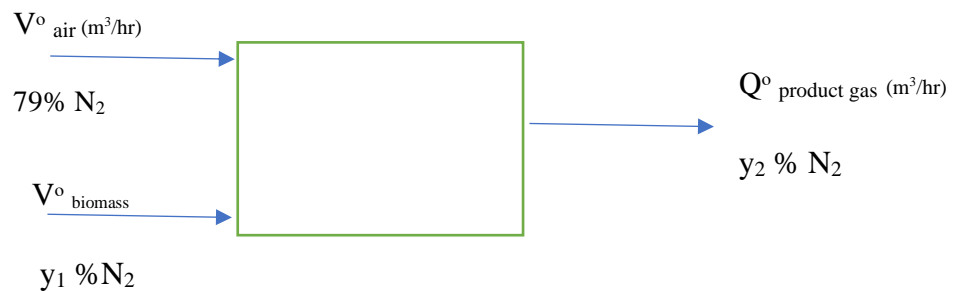
**Equation 2-5 High Heating value for the product gas**

**Table 2-5 The standard heating values of H<sub>2</sub>, CO, and CH<sub>4</sub>.**

Gases	H <sub>2</sub>	CO	CH <sub>4</sub>
HHV (MJ/Nm <sup>3</sup> )	12.74	12.63	39.82
LHV (MJ/Nm <sup>3</sup> )	10.78	12.63	35.88

### 2.4.3 Gas yield

Based on the law of conservation of mass, the yield of product gas was calculated based on the nitrogen content in the gas exiting the reactor. The air supplied to the reactor contains 79% N<sub>2</sub> and 21% O<sub>2</sub>. While oxygen is being consumed in the reactions, the nitrogen is an inert gas, with a constant flow rate. The nitrogen exists at a very low concentration in the feedstock (0-1.5 wt%), therefore it can be neglected. The gas yield was calculated by using the nitrogen concentration acquired from the Micro-GC analysis as an internal standard.



### **3. Results and discussion**

#### **3.1 Gasification of pure biomass**

##### **3.1.1 Gasification of pure birch sawdust (temperature variation)**

The first group of experimental runs were meant to study the temperature effect on the gasification process to verify the reliability of the system, and standardize the temperature, and the equivalence ratio of the remaining experimental runs. Silica sand was used as a bed material for these runs. Temperature of the bed was raised from 700 °C to 850 °C before introducing the fuel to the reactor, the air was heated to 200-300 °C. The flow rate of the air was adjusted and measured to keep the equivalence ratio at the optimum range of 17-20%. The produced gas was collected in Tedlar® gas sampling bags to be analyzed using the micro-GC. Samples were collected after 20 to 30 minutes from the start of feeding. The readings from micro-GC were averaged.

Table 3-1 summarizes the produced gases at 700 °C; hydrogen, carbon monoxide, carbon dioxide, and methane had concentrations of 7.1%, 18.4%, 11.3% and 4.8% respectively. When the temperature was raised to 850 °C, the hydrogen concentration doubled due to the endothermic reactions, such as water gas (R6), Methane steam reforming (R9), and Bourdourd reaction (R13) as shown in Table 1-2, by shifting the chemical equilibrium towards the formation of products according to Le Chatelier's principle. A significant increase in the carbon monoxide and the heating value were observed.

The rise of temperature favored the formation of H<sub>2</sub> and decreased the formation of hydrocarbons, tars and char is in agreement with other researchers findings [67]. This is attributed to the occurrence of the endothermic reactions and the suppression of the exothermic reactions.

The produced gases from 100% BSD had higher heating values ranging from 4.8 to 7 MJ/Nm<sup>3</sup>. The main contributors to the heating value from the BSD are the methane and the carbon monoxide

which represented 4.8-5.4% and 18.4-25.9% (%vol) respectively, while hydrogen was measured to range from 7.1 to 12.8%. The H<sub>2</sub>/CO ratio in the produced gases from 100% woody biomass increased from 0.38 to 0.49 as temperature increased. The gas composition is in alignment with other researchers as shown in Table 3-5.

**Table 3-1 Effect of Temperature on gas composition from pure BSD**

	BSD 700C 26%	BSD 800C 21%	Kim et al. [104]	Lucio and Maria [105]
H <sub>2</sub> (%)	7.1	12.8	12.7	12
CO (%)	18.4	25.9	15.5	17
CH <sub>4</sub> (%)	4.8	5.4	5.7	4
CO <sub>2</sub> (%)	11.3	8.2	15.9	15
LHV (MJ/Nm <sup>3</sup> )	5.2	7.0	-	6.15
HHV (MJ/Nm <sup>3</sup> )	5.5	7.4	-	

### 3.1.2 Gasification of pure rice husk (temperature variation)

The rice husk was used as the feedstock over the silica sand bed. The airflow rate was kept constant for the three runs in order to keep the equivalence ratio steady at 18.5%. The gas composition has been measured over the temperature range 750-850 °C at a constant equivalence ratio. The measured product gas concentrations are shown in Table 3-2

**Table 3-2 Rice husk (variation of Temperature)**

Temp (°C)	This study			Behainne et al. [106]*	Makwana et al. [107]**
	750	800	850		
H <sub>2</sub> (%)	4.35	6.82	9.95	3.5-6.8	6
CO (%)	12.18	12.68	18.56	8-14	18
CH <sub>4</sub> (%)	2.45	3.76	4.35	2.8-4.09	3
CO <sub>2</sub> (%)	5.01	4.95	4.92	10-14.5	-
LHV (MJ/Nm <sup>3</sup> )	2.89	3.69	4.98		3.9 <sub>(HHV)</sub>
H <sub>2</sub> /CO	0.36	0.43	0.4	0.35-0.39	

\*ER=0.2-0.36

\*\*ER =0.3

It is observed that the overall gasification reactions and hydrogen production increased at higher temperature, consequently the heating value increased. The hydrogen and the heating value were observed to be doubled when the temperature was raised from 750 °C to 850 °C, while CO<sub>2</sub> stabilized at the same value. The heating values of the produced gas which has been calculated based on the empirical correlation given in Equation 2-5 on page 34, showed the same trend as it is a reflection of the three combustible components H<sub>2</sub>, CH<sub>4</sub>, and CO.

The high temperature increased the rate of endothermic reactions such as the water gas reaction and Boudouard reaction, by shifting the chemical equilibrium towards the formation of products

according to Le Chatelier's principle. Besides, a significant increase in the carbon monoxide and the heating value was observed [67][108].

During the gasification of the rice husk, a larger amount of ash left over was observed than that found during birch sawdust gasification. This can be predicted from the proximate analysis results which indicated in Table 2-1, where the ash percentage was 16.8% for the rice husk compared to 1% in the birch sawdust. The existence of the volatile matter of biomass, which is the portion that can convert into gases relatively easier than the fixed carbon, enhanced the solid to gas conversion at high temperatures. This can be anticipated from the proximate analysis. In other studies when compared the volatile matter content of coal (<35%) to that of biomass which has higher volatile matter (>50%) [50][66] the gas yield was noticed to be higher.

Many researchers observed an increase in the gas conversion with the temperature. For instance, Pinto et. al. [67] steam gasified the PE waste with pinewood feedstock at a ratio of 10%  $w_{PE}/w_{sample}$  over a temperature range from 740 °C to 885 °C; he noticed a 100% increase in the gas yield while only 65% rise of the yield when gasified the PE at ratio 40% of the feedstock. He noticed an increase in conversion of feedstock into a gas, and hydrogen content increased as the temperature increased when mixing the pine wood with 20%.. Narvaez et. al. [109] mentioned a 100% jump in the hydrogen from 5 to 10% when the temperature increased from 700 °C to 850 °C.

We conclude that the gasification temperature has a determinantal effect on the produced gas.

Although both exothermic and endothermic reactions occur simultaneously, the higher the

temperature, the higher carbon conversion. Moreover, The more volatile content of the fuel the higher the yield and the efficiency.

Therefore, The addition of plastics (LDPE and HDPE) to the birch sawdust and the rice husk is promising

### 3.2 Co-gasification of LDPE pre-mixed with birch sawdust

The study of the effect of the LDPE ratio in the feedstock has been done by gasification of birch sawdust pre-mixed with LDPE at three different percentages: 15%, 30%, and 50% (by wt% ). Silica sand was used as a bed material for these runs. The temperature of the bed and the equivalence ratio of air were kept constant at 850 °C and 16-17%, respectively, due to the satisfactory quality of product gas obtained from the previous runs that match the literature suggested optimum temperature.

As observed from Table 3-3, a consistent increase in hydrogen and methane was observed while CO fell continuously upon the addition of LDPE to the birch sawdust. When we compare the gas from the 15% LDPE to the 50%, it is obvious that hydrogen increased 50% to reach 12% by volume of the produced gas. CO decreased from 8.8 % to 4.9%, which resulted in the H<sub>2</sub>/CO ratio increasing from 0.9 at 15% LDPE to 2.4 at 50% LDPE,. The rise of the highly combustible gases (H<sub>2</sub> & CH<sub>4</sub>) increased the LHV from 2.8 to 4.1MJ/Nm<sup>3</sup> which was less than the sharp rise in the hydrogen due to the offset effect that happened by the drop of the CO which decreased by approximately 68%.

**Table 3-3 Effect of LDPE ratio premixed with birch sawdust as feedstock**

LDPE %	LDPE pre-mixed in feedstock		
	15%	30%	50%
H <sub>2</sub> (%)	7.9	13.91	12.04
CO (%)	8.86	13.82	4.94
CH <sub>4</sub> (%)	2.5	7.03	6.23
CO <sub>2</sub> (%)	1.76	0.82	1.13
LHV (MJ/Nm <sup>3</sup> )	2.88	5.77	4.16
H <sub>2</sub> /CO	0.9	1.01	2.4

That behavior aligned well with what Pinto et. al. [67] observed when the PE was added at 40-60 wt%; Hydrogen was doubled and CO decreased by approximately 25% compared to the pure biomass. He noted that the  $H_2/CO$  and  $H_2/CO_2$  ratios were higher as the ratio of the polyethylene increased, which was attributed to the polymer cracking and possible consumption of  $CO_2$  by the Bourdouard reaction. The increase in  $CH_4$  is attributed to the methanation reaction, which is promoted due to the high concentration of Hydrogen.

It has been observed by other researchers who studied mixtures of coals, plastics, and wood, that the addition of plastics enhances the specific energy of the produced gas (energy of the produced gas / fuel mass rate) which is attributed to the increase of both  $CH_4$  and the light hydrocarbons [63]. The thermal cracking of the plastic polymer structure into large fragments is expected to be the reason behind producing saturated and unsaturated hydrocarbons which in turn crack into hydrogen and light hydrocarbon, and resulted in an increased yield. Zhu et al. [110] noticed the product gas's calorific value is higher when more polyethylene was added to the beechwood which was related to a higher calorific value of the feedstock itself as the polyethylene is almost three times that of the wood's calorific value. The hydrogen content was higher. As well as the tars content which is related to the high volatile content in the plastics.

The higher  $H_2$  content in the product gas and the higher  $H_2$  to CO concentration is a feature that is favoured in different applications such as hydrogen production, methanol, and higher hydrocarbon weight fuel production via Fischer-Tropsch. The tar content has been noticed to increase with the plastic addition in this study (photos were added in Appendix B) which was the same observation by Zhu et. al [110] who observed less tar produced from the wood gasification.

### 3.3 Effect of various bed materials on co-gasification of plastics and biomass

#### 3.3.1 Effect of olivine as a bed material on co-gasification of plastics and biomass

The effect of olivine as a bed material has been studied by gasification of pre-mixed biomass (birch sawdust BSD and rice husk RH) with plastics (LDPE and HDPE) at a constant ratio of 50%  $W_{\text{plastic}}/W_{\text{sample}}$  (Figure 3-1 is a visual representation of different mixtures). All experiments took place at 850 °C and with an airflow rate 20 scfh. The feedstock flow rate was adjusted to fix the equivalence ratio at 17-18% according to the fuel composition. Olivine sand was used for all experiments for birch sawdust and another fresh olivine sand was used for rice husk experiments. The weight of the bed ranged from 2,500 g to 2,800 g offering 23-26 cm bed height. Silica sand runs were considered as the base case.

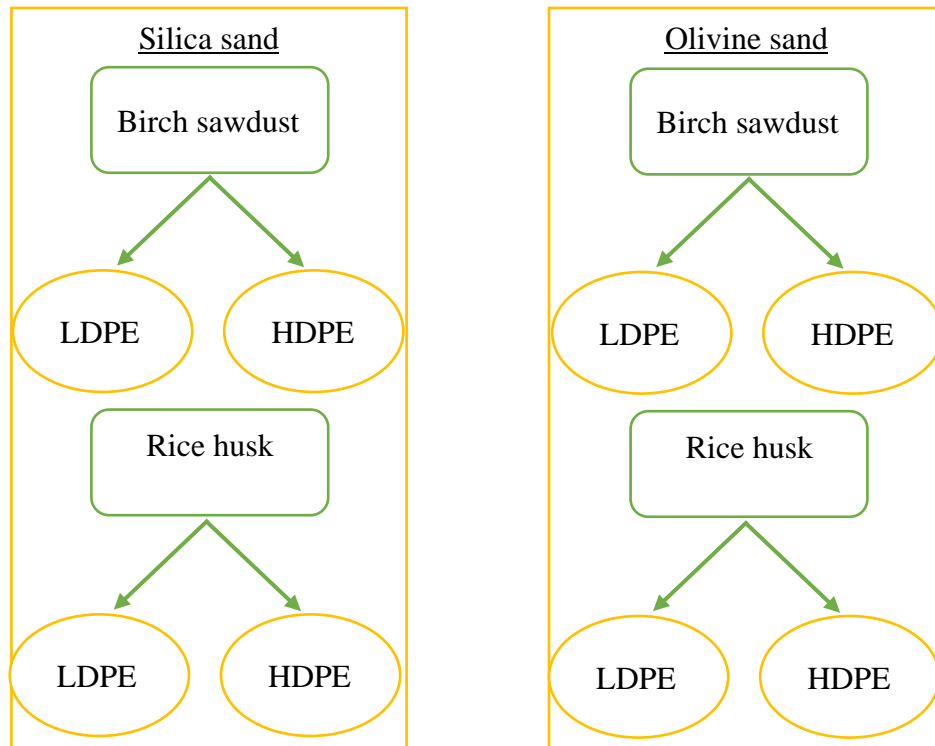
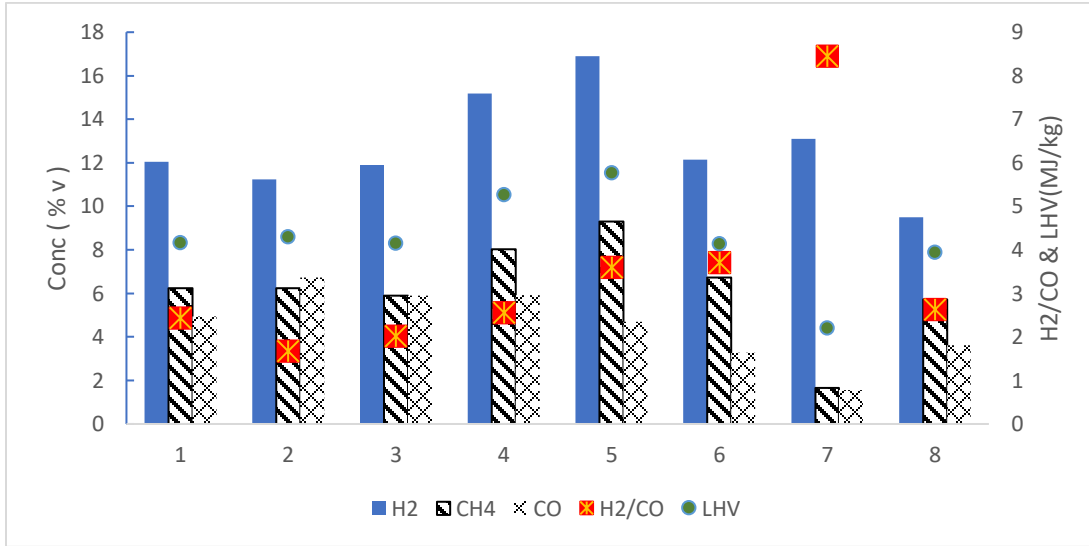


Figure 3-1 Different batches of biomass-plastic mix at ratio 50%

The hydrogen concentration of the silica sand runs was steady for each feedstock combination at the same operating parameters. In contrast, for the olivine runs, the high production of hydrogen at the first runs (850 °C bed temperature and air flow rate 20 scfh) due to the catalytic activity on the olivine surface that enhanced the breakage of the C-H bond of the feedstock structure. The rise in hydrogen was followed by a consecutive drop of its concentration in the product gas due to the loss of olivine's catalytic activity (Notice runs 6 - 8 in Figure 3-2 and runs 4 - 6 in Figure 3-3) The carbon monoxide followed the same pattern of deficiency as the hydrogen, which can be related to the deposition of carbon on the olivine surface which can be examined by CHN-S or a thermogravimetric analysis (in future investigation).

The gas yield was calculated for the runs based on molar balance of nitrogen. The gas yield from the mixture of BSD with plastics decreased from 1.4-1.5 to 1.2-1.3 (Nm<sup>3</sup>/kg feedstock) when used the silica sand and the olivine, respectively. While the rice husk mixtures yield was less than that of the BSD mixtures at an average of at 1.2-1.3(Nm<sup>3</sup>/kg feedstock)



**Figure 3-2 Product gas (dry) components concentration from BSD mixed with plastics using silica and olivine ( runs 1-4 silica sand bed, 5-8 olivine bed, runs 1,2,5,6 BSD+LDPE runs 3,4,7,8 BSD+HDPE)**

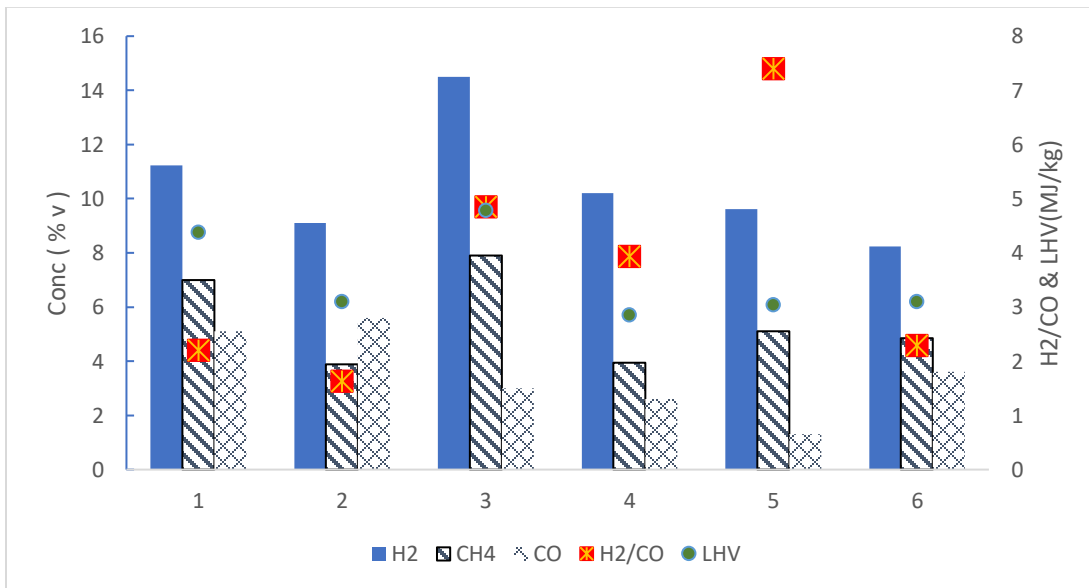


**Figure 3-3 Product gas (dry) components concentration using silica and olivine (runs 1-2 Silica sand bed, 3-6 olivine bed, runs 1,5,6 RH+LDPE runs 2,3,4 RH+HDPE)**

The behaviour of declining hydrogen concentration was noticed while gasification of plastic waste [111]. It is believed that the olivine, which has a proven catalytic effect, is capable of enhancing the plastic thermal degradation resulting in a higher gas yield and more hydrogen productivity. The catalytic effect degrades over time because the metals started depletion into the hydrocarbons formed on the surface and escapes with the fines. To maintain the highest hydrogen concentration in the produce gas, replenishment of the olivine is needed to have an uninterrupted operation. Devi et al. [93] compared the tar reformation that occurred by calcined dolomite versus the untreated olivine. Although the dolomite addition to the sand bed was more reactive in decomposing 90% of tar, the olivine addition converted 70%. It was noted that the olivine resistance to attrition is higher and was seen as promising bed material. An interesting technique was done by Sergio et al. [112], where the used olivine (used as a catalytic filter in the freeboard) performed better than the fresh olivine in steam gasification reaction attributed to a positive effect of a char particles on the tar conversion. It is noticed that hydrogen yield increased by 20% and the tar dropped by 87% even after 4 hrs of operation.

The positive insight in all experiments is that the product gas has  $H_2/CO$  ratio greater than 1, which qualifies the gas to be used in hydrogen dependant applications. However, the noticeable amount of ash produced during rice husk gasification is a factor that limits the temperature of the process as it might cause sintering [113]. Park et al. [57] noticed the agglomeration caused during rice husk gasification and studied its adverse effect on the air hydrodynamics which caused a drop in the gas quality. Different structures of agglomerates are shown in Figure 3-4

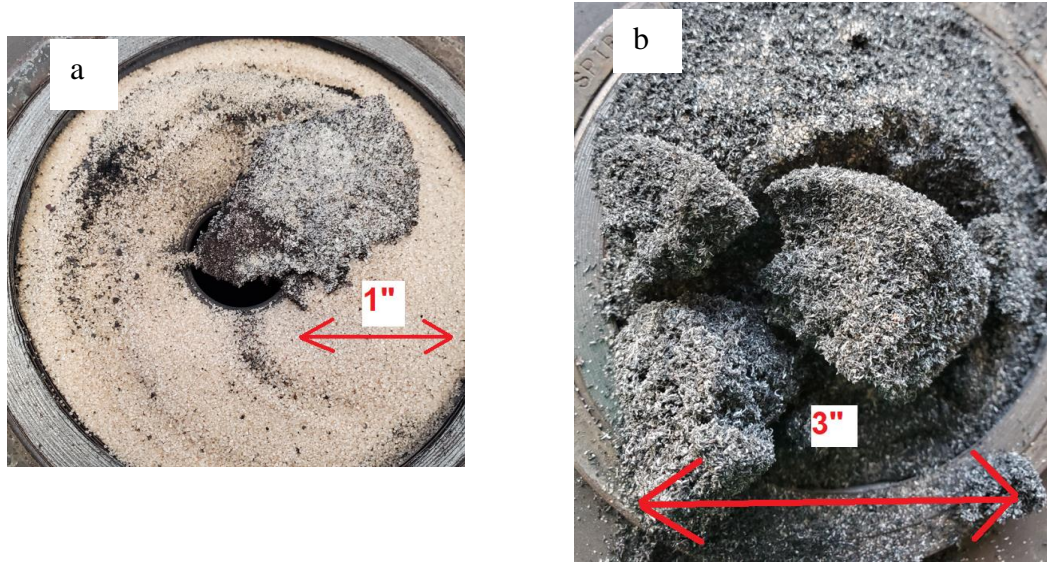


**Figure 3-4 Ash agglomeration in sand beds a-BSD+LDPE b-RH-LDPE**

**Table 3-4 Examples of agglomerate's structure from rice husk**

Sample	SiO <sub>2</sub>	MgO	Fe <sub>2</sub> O <sub>3</sub>	K <sub>2</sub> O	Al <sub>2</sub> O <sub>3</sub>	CaO	Cr <sub>2</sub> O <sub>3</sub>	MnO	P <sub>2</sub> O <sub>5</sub>	others
1	70.19	16.71	6.25	2.41	1.72	.87	.96	0.43	0.13	<0.1
2	64.43	22.05	7.7	1.2	2	0.73	1.03	0.41	0.13	<0.1
3	92.43	0.95	0.48	4.11	0.22	1.18	0.07	0.27	0.13	<0.1

### **3.3.2 Effect of red mud as a bed material on co-gasification of plastics and biomass**

The red mud, which is rich in iron and aluminum compounds (as mentioned in section 2.3.2 ), is considered an undesirable waste of bauxite residue.

It has been used as a bed material for the 3 types of mixtures mentioned in Figure 3-5. The experiments were done at the same temperature 850 °C. The equivalence ratio was kept constant at 16-17%. Product gas, rich in hydrogen and carbon monoxide, was obtained and summarized in Figure 3-6

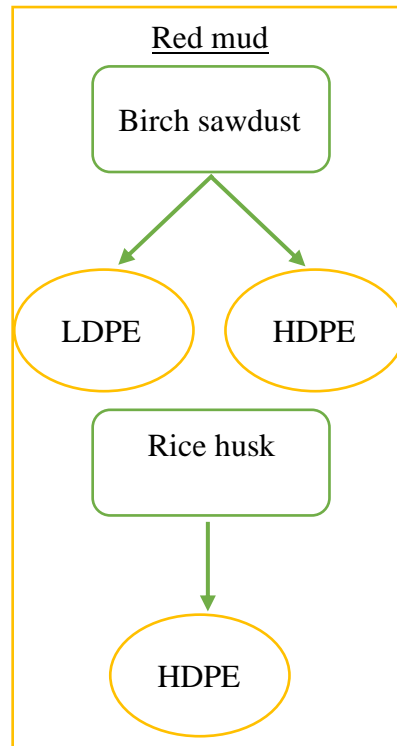


**Figure 3-5 Red mud feedstock combinations (50%biomass-50%plastic)**

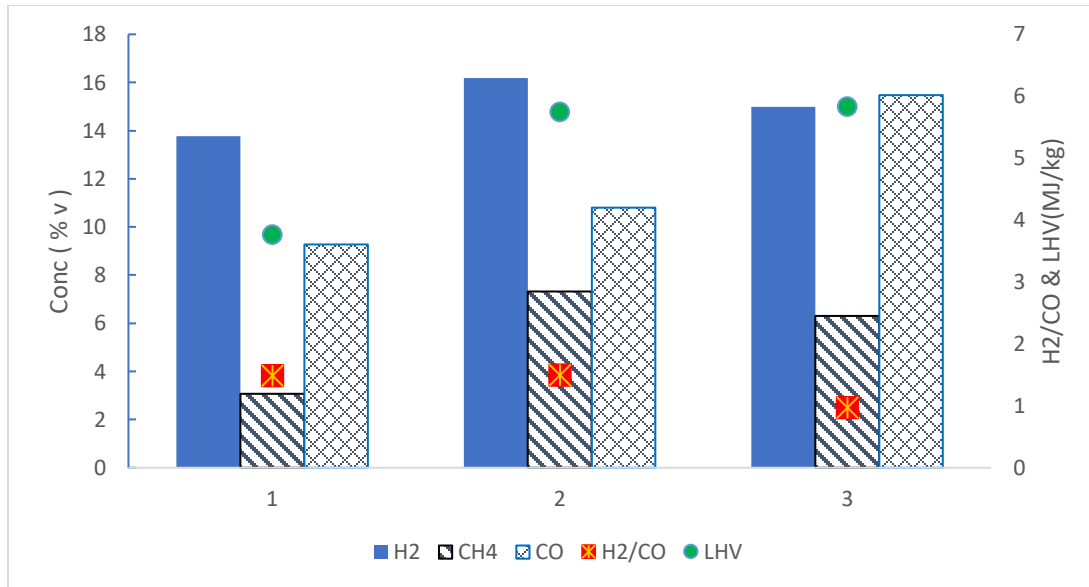


**Figure 3-6 Product gas (dry) components concentration using red mud (run1: BSD+LDPE, run2: BSD+HDPE, run3: RH+LDPE)**

The hydrogen produced using red mud as bed material is generally higher than that produced from silica and olivine. The birch sawdust mixed with HDPE yielded a higher concentration of H<sub>2</sub> and CO gas than the birch sawdust-LDPE mix. The H<sub>2</sub>/CO ratio is more than 1 for all runs which is suitable for internal combustion engines use or fuel cell applications.

Chen et al.[99] used the red mud for tar reforming and considered the naphthalene as a model compound. They treated the red mud in three different ways before testing; calcination at 600°C for 2 hrs, reduction using H<sub>2</sub>-N<sub>2</sub> mixture, and HCl activation. While the red mud pre-exposure to H<sub>2</sub> enhanced the tar decomposition to yield lighter hydrocarbon and hydrogen. It was mentioned that the presence of CO within the reducing gas caused a coking problem then the process had to stop after 4 hrs. I believe that in this study the red mud was reduced by the gasification product gas (mainly H<sub>2</sub>) consequently the catalytic effect of the iron compounds contributed to producing

more hydrogen. However the test was done for 30-40 minutes only, so we cannot agree or disagree with the fact of losing the red mud surface activity due to the CO existence or coke deposition.

**Table 3-5 Gasification conditions and gas composition from literature**

	Nam et al. [114]	Park et al. [57]	Kim et al. [104]	Zaccariello and Mastellone [105]	Zaccariello and Mastellone [105]	Narvaez et al. [109]	Arena et al. [115]	Mastral et al. [116]
Feedstock	Hardwood pellets	Rice husk	Wood	Wood	Recycled Plastic	Pine wood	MWP1*	HDPE
Feedstock HHV MJ/kg	19.9	-	18	18.4	42.69	18-18.4	42.7	
Temp (°C)	850	700-850	750	870	877	800	887	850
ER	0.23	0.2	0.19	0.25	0.24	0.26	.248	
Bed material	Silica sand	Silica sand	Silica sand	Silica sand	Silica sand	Silica sand	olivine	Silica sand
H <sub>2</sub> (%)	6.8	5	16.5	12.16	9.2	9.5	5.9 **	15
CO (%)	15	22	16.1	17.13	4.9	13	4.5 **	-
Product gas LHV (MJ/Nm <sup>3</sup> )	7.7	5.8	5.7	6.15	7.9	4.5		
CGE %	65	41-62						

\*MPW: mixed plastic waste

\*\*species concentrations in the produce gas including Nitrogen

## **4. Conclusions, novelty statement, and recommendations**

### **4.1 Conclusions and novelty**

As the world population continues to increase, the use of plastic products and disposal volumes will reach higher numbers. Food consumption will follow the same trend. The energy and chemicals contained in the discarded plastic and agricultural wastes need to be recovered in an environmental, economical way. In this thesis, LDPE and HDPE have been mixed with biomass waste and gasified in a bubbling fluidized bed at 850 °C. The mixed feedstocks have produced a low calorific value of product gas (syngas 3-6 MJ/Nm<sup>3</sup>) that is rich in valuable hydrogen gas.

In this study, we utilized a fluidized bed reactor for the gasification of biomass. The feeding problem of plastics was overcome by mixing plastics with biomass which enhanced the flowability of the feedstock. This technique might be applicable in other reactor configurations and prevent feed melting/sintering before reaching the reactor [69]. An optimum amount of biomass is needed otherwise more biomass will decrease the gasification temperature leading to less hydrogen production and more methanation reaction [117]. The effect of using different bed materials on the concentration of hydrogen in the syn gas was studied. Olivine can be utilized as a catalytic bed material and an increase in the hydrogen concentration was noticed, however the loss of the active sites mandates the replenishment of the bed accordingly. Also, red mud showed proper catalytic behaviour which was close to the olivine. The advantage of red mud usage is utilizing industrial waste from the aluminum production, which is considered a liability for that industry as it imposes storage problems. Consequently, reducing the red mud activity through obtaining it in a fully oxidized form after the gasification process, will make its disposal safer in the oxidized form but the drawback is that attrition of the red mud that occurred in the bed resulted in more dust which mandates more strict dust control measures to prevent any environmental air pollution [118].

## **4.2 Recommendations for further investigation and equipment upgrading**

### **4.2.1 Feedstock**

The used feedstock in this study was biomass waste and raw Low-density polyethylene pellets and raw high-density polyethylene pellets. It's recommended to use waste LDPE/HDPE separated or mixed to test the effect of processing plastics (such as a packaging industry waste) on the product gas. Mixed plastics would be preferred from a practical point of view to save the costs associated with the separation process.

### **4.2.2 Olivine**

Olivine presented a good catalytic effect for a certain time but the formation of the coke eventually covers the active sites, so it is recommended to test the gasification process using calcined olivine and also adding fresh olivine might help. It is advisable to examine for longer time to make sure the performance will stay steady.

### **4.2.3 Red mud**

Red mud is a cheap source of catalytic bed material due to the high metal content, especially iron. The red mud has been dried, crushed, then sieved before being used. During the bed fluidization, the particles showed attrition behaviour due to friction between particles so deval attrition test is suggested to quantify the attrition. A study of red mud activation using acid (HCl or HNO<sub>3</sub>) might be incorporated[119] due to the dissociation/leaching of sintering particles (sodium aluminosilicate). Dust collecting system may need modification to handle finer particles and improve maintainability or use the red mud as a catalytic filter in the freeboard.

#### **4.2.4 Particulate**

The current cyclone needs to be modified/changed with a removable top cyclone for ease of maintenance. The use of thimble filter may be considered to in the tar/gas sampling to avoid carry over of any solid particle.

#### **4.2.5 Tar**

Tar is one of the main setback challenges in utilizing small-medium scale gasification. Tar has been noticed to stick to the wall of the piping downstream the reactor due to the wide gradient of the temperature post the reactor which prevented proper tar exit.

For the system used in this context, a tar sampling system is needed to quantify the amount of tar and analyze the compounds that are being formed during the process to address the catalysis in a more precise way. Activated carbon can be also be considered in treating the tar [120].

## Reference

- [1] M. Roser and H. Ritchie, “Energy mix,” *Our World in Data*, 2022. <https://ourworldindata.org/energy-mix> (accessed Jan. 17, 2022).
- [2] N. U. Benson, D. E. Bassegy, and T. Palanisami, “COVID pollution: impact of COVID-19 pandemic on global plastic waste footprint,” *Heliyon*, vol. 7, no. 2, p. e06343, 2021, doi: 10.1016/j.heliyon.2021.e06343.
- [3] S. Nanda and F. Berruti, “Thermochemical conversion of plastic waste to fuels: a review,” *Environ. Chem. Lett.*, no. 0123456789, 2020, doi: 10.1007/s10311-020-01094-7.
- [4] “Closed Loop Partners Launches Multi-Million Dollar Circular Plastics Fund with Dow, LyondellBasell, & NOVA Chemicals to Accelerate Investment in Plastics Recycling Infrastructure,” 2021. <https://www.novachem.com/media-center/news-releases/closed-loop-partners-launches-multi-million-dollar-circular-plastics-fund-with-dow-lyondellbasell-nova-chemicals-to-accelerate-investment-in-plastics-recycling-infrastructure/> (accessed Oct. 10, 2021).
- [5] S. M. Al-Salem, A. Antelava, A. Constantinou, G. Manos, and A. Dutta, “A review on thermal and catalytic pyrolysis of plastic solid waste (PSW),” *J. Environ. Manage.*, vol. 197, no. 1408, pp. 177–198, 2017, doi: 10.1016/j.jenvman.2017.03.084.
- [6] O. E. Ezenkwa, A. Hassan, and S. A. Samsudin, “Influence of different surface treatment techniques on properties of rice husk incorporated polymer composites,” *Rev. Chem. Eng.*, vol. 37, no. 8, pp. 907–930, Nov. 2020, doi: 10.1515/REVCE-2019-0027/ASSET/GRAPHIC/J\_REVCE-2019-0027\_FIG\_003.JPG.
- [7] H. Ellis-Petersen, “Delhi’s smog blamed on crop fires – but farmers say they have little choice,” 2019. <https://www.theguardian.com/world/2019/nov/08/indian-farmers-have-no-choice-but-to-burn-stubble-and-break-the-law> (accessed Jan. 17, 2022).
- [8] R. Pardikar, “How to beat air pollution? Stop burning the fields,” 2018. <https://www.theguardian.com/world/2018/oct/16/how-new-tech-is-helping-india-farmers-tackle-air-pollution-smog> (accessed Jan. 17, 2022).
- [9] S. P. Wickramage, J. Rajaratne, and M. Udupihille, “Factors affecting respiratory function of rice millers in Anuradhapura district,” *Anuradhapura Med. J.*, vol. 11, no. 1, p. 4, Sep. 2018, doi: 10.4038/AMJ.V11I1.7644.
- [10] T. Ghosh, S. Gangopadhyay, and B. Das, “Prevalence of respiratory symptoms and disorders among rice mill workers in India,” doi: 10.1007/s12199-014-0384-8.
- [11] S. S. Siwal *et al.*, “Recovery processes of sustainable energy using different biomass and wastes,” *Renew. Sustain. Energy Rev.*, vol. 150, no. June, p. 111483, 2021, doi: 10.1016/j.rser.2021.111483.
- [12] J. Cai *et al.*, “Review of physicochemical properties and analytical characterization of lignocellulosic biomass,” *Renew. Sustain. Energy Rev.*, vol. 76, no. October 2016, pp. 309–322, 2017, doi: 10.1016/j.rser.2017.03.072.

- [13] S. Chieng, “Harnessing bioenergy and high value-added products from rice.pdf,” 2020.
- [14] N. T. Kim Oanh *et al.*, “Particulate air pollution in six Asian cities: Spatial and temporal distributions, and associated sources,” *Atmos. Environ.*, vol. 40, no. 18, pp. 3367–3380, 2006, doi: 10.1016/j.atmosenv.2006.01.050.
- [15] U. EPA, “Timeline of Particulate Matter (PM) National Ambient Air Quality Standards (NAAQS),” *Particulate Matter (PM) Pollution*, 2012. <https://www.epa.gov/pm-pollution/timeline-particulate-matter-pm-national-ambient-air-quality-standards-naaqs> (accessed Nov. 14, 2021).
- [16] C. W. Purnomo, W. Kurniawan, and M. Aziz, “Technological review on thermochemical conversion of COVID-19-related medical wastes,” *Resources, Conservation and Recycling*, vol. 167. 2021, doi: 10.1016/j.resconrec.2021.105429.
- [17] I. Tiseo, “Global plastic production 1950-2020,” 2022. <https://www.statista.com/statistics/282732/global-production-of-plastics-since-1950/>.
- [18] P. Plastics Europe, “Plastics - the Facts 2021,” 2021. [Online]. Available: <https://plasticseurope.org/wp-content/uploads/2021/12/Plastics-the-Facts-2021-web-final.pdf>.
- [19] R. Geyer, B. Kuczenski, T. Zink, and A. Henderson, “Common Misconceptions about Recycling,” *J. Ind. Ecol.*, vol. 20, no. 5, pp. 1010–1017, 2016, doi: <https://doi.org/10.1111/jiec.12355>.
- [20] E. R. K. Neo, G. C. Y. Soo, D. Z. L. Tan, K. Cady, K. T. Tong, and J. S. C. Low, “Life cycle assessment of plastic waste end-of-life for India and Indonesia,” *Resour. Conserv. Recycl.*, vol. 174, no. July, p. 105774, 2021, doi: 10.1016/j.resconrec.2021.105774.
- [21] E. D. Lavric, A. A. Konnov, and J. De Ruyck, “Dioxin levels in wood combustion—a review,” *Biomass and Bioenergy*, vol. 26, no. 2, pp. 115–145, Feb. 2004, doi: 10.1016/S0961-9534(03)00104-1.
- [22] I. Vollmer *et al.*, “Beyond Mechanical Recycling: Giving New Life to Plastic Waste,” *Angew. Chemie - Int. Ed.*, vol. 59, no. 36, pp. 15402–15423, 2020, doi: 10.1002/anie.201915651.
- [23] I. Zeb *et al.*, “In-situ microaeration of anaerobic digester treating buffalo manure for enhanced biogas yield,” *Renew. Energy*, vol. 181, pp. 843–850, Jan. 2022, doi: 10.1016/J.RENENE.2021.09.089.
- [24] C. J. Rivard *et al.*, “Anaerobic Digestion of Municipal Solid Waste Utility of Process Residues as a Soil Amendment,” 1995.
- [25] Y. K. Choi, T. Y. Mun, M. H. Cho, and J. S. Kim, “Gasification of dried sewage sludge in a newly developed three-stage gasifier: Effect of each reactor temperature on the producer gas composition and impurity removal,” *Energy*, vol. 114, pp. 121–128, 2016, doi: 10.1016/j.energy.2016.07.166.
- [26] J. Merrylin, S. A. Kumar, S. Kaliappan, I.-T. Yeom, and J. R. Banu, “Biological

- pretreatment of non-flocculated sludge augments the biogas production in the anaerobic digestion of the pretreated waste activated sludge,” *Environ. Technol.*, vol. 34, no. 13–14, pp. 2113–2123, Jul. 2013, doi: 10.1080/09593330.2013.810294.
- [27] V. A. Schommer, B. M. Wenzel, and D. J. Daroit, “Anaerobic co-digestion of swine manure and chicken feathers: Effects of manure maturation and microbial pretreatment of feathers on methane production,” *Renew. Energy*, vol. 152, pp. 1284–1291, Jun. 2020, doi: 10.1016/J.RENENE.2020.01.154.
- [28] J. D. Marin-Batista, J. A. Villamil, S. V. Qaramaleki, C. J. Coronella, A. F. Mohedano, and M. A. d. la Rubia, “Energy valorization of cow manure by hydrothermal carbonization and anaerobic digestion,” *Renew. Energy*, vol. 160, pp. 623–632, Nov. 2020, doi: 10.1016/J.RENENE.2020.07.003.
- [29] A. Abraham *et al.*, “Pretreatment strategies for enhanced biogas production from lignocellulosic biomass,” *Bioresour. Technol.*, vol. 301, p. 122725, Apr. 2020, doi: 10.1016/J.BIORTECH.2019.122725.
- [30] G. Kumar *et al.*, “A comprehensive review on thermochemical, biological, biochemical and hybrid conversion methods of bio-derived lignocellulosic molecules into renewable fuels,” *Fuel*, vol. 251, no. April, pp. 352–367, 2019, doi: 10.1016/j.fuel.2019.04.049.
- [31] C. A. García-Velásquez and C. A. Cardona, “Comparison of the biochemical and thermochemical routes for bioenergy production: A techno-economic (TEA), energetic and environmental assessment,” *Energy*, vol. 172, pp. 232–242, Apr. 2019, doi: 10.1016/J.ENERGY.2019.01.073.
- [32] V. Dhyani and T. Bhaskar, “A comprehensive review on the pyrolysis of lignocellulosic biomass,” *Renew. Energy*, vol. 129, pp. 695–716, 2018, doi: 10.1016/j.renene.2017.04.035.
- [33] J. Watson, Y. Zhang, B. Si, W. T. Chen, and R. de Souza, “Gasification of biowaste: A critical review and outlooks,” *Renew. Sustain. Energy Rev.*, vol. 83, no. December 2016, pp. 1–17, 2018, doi: 10.1016/j.rser.2017.10.003.
- [34] A. R. K. Gollakota, N. Kishore, and S. Gu, “A review on hydrothermal liquefaction of biomass,” *Renew. Sustain. Energy Rev.*, vol. 81, pp. 1378–1392, Jan. 2018, doi: 10.1016/J.RSER.2017.05.178.
- [35] A. Pandey, ;, and Thallada Bhaskar, *Recent Advances in Thermochemical Conversion of Biomass*. 2015.
- [36] N. D. Montiel-Bohórquez and J. F. Pérez, “Energy valorization strategies of fallen leaves and woody biomass in a based downdraft gasification-engine power plant,” *Sustain. Energy Technol. Assessments*, vol. 49, no. October 2021, 2022, doi: 10.1016/j.seta.2021.101749.
- [37] D. Sofia, P. Coca Llano, A. Giuliano, M. Iborra Hernández, F. García Peña, and D. Barletta, “Co-gasification of coal–petcoke and biomass in the Puertollano IGCC power plant,” *Chem. Eng. Res. Des.*, vol. 92, no. 8, pp. 1428–1440, Aug. 2014, doi: 10.1016/J.CHERD.2013.11.019.
- [38] G. Guan *et al.*, “High-density circulating fluidized bed gasifier for advanced IGCC/IGFC—

- Advantages and challenges,” *Particuology*, vol. 8, no. 6, pp. 602–606, Dec. 2010, doi: 10.1016/J.PARTIC.2010.07.013.
- [39] D. C. Spath, P L;Dayton, “Preliminary Screening -- Technical and Economic Assessment of Synthesis Gas to Fuels and Chemicals with Emphasis on the Potential for Biomass-Derived Syngas,” 2003. doi: 10.2172/15006100.
- [40] M. P. Relations, “GE Gas Engines Turning Waste Wood into Cleaner Energy for Italy,” 2011. <https://www.ge.com/news/press-releases/ge-gas-engines-turning-waste-wood-cleaner-energy-italy> (accessed Feb. 20, 2022).
- [41] M. M. Win, M. Asari, R. Hayakawa, H. Hosoda, J. Yano, and S. ichi Sakai, “Characteristics of gas from the fluidized bed gasification of refuse paper and plastic fuel (RPF) and wood biomass,” *Waste Manag.*, vol. 87, pp. 173–182, 2019, doi: 10.1016/j.wasman.2019.02.002.
- [42] E. Wim van Swaaij, Sascha Kersten, and Wolfgang Palz, *Biomass Power for the World: Transformations to Effective Use*. 2015.
- [43] N. Mahinpey and A. Gomez, “Review of gasification fundamentals and new findings: Reactors, feedstock, and kinetic studies,” *Chem. Eng. Sci.*, vol. 148, pp. 14–31, Jul. 2016, doi: 10.1016/J.CES.2016.03.037.
- [44] P. Basu, *Biomass Gasification and Pyrolysis*. 2010.
- [45] A. Andersson, “Effects of bed particle size on heat transfer in circulating fluidized bed boilers,” vol. 87, pp. 239–248, 1996.
- [46] A. Kumar, D. D. Jones, and M. A. Hanna, “Thermochemical biomass gasification: A review of the current status of the technology,” *Energies*, vol. 2, no. 3, pp. 556–581, 2009, doi: 10.3390/en20300556.
- [47] V. Claude, C. Courson, M. Köhler, and S. D. Lambert, “Overview and Essentials of Biomass Gasification Technologies and Their Catalytic Cleaning Methods,” *Energy and Fuels*, vol. 30, no. 11. American Chemical Society, pp. 8791–8814, Nov. 17, 2016, doi: 10.1021/acs.energyfuels.6b01642.
- [48] S. Safarian, R. Unnþórsson, and C. Richter, “A review of biomass gasification modelling,” *Renew. Sustain. Energy Rev.*, vol. 110, no. May, pp. 378–391, 2019, doi: 10.1016/j.rser.2019.05.003.
- [49] J. F. Pérez, A. Melgar, and F. V. Tinaut, “Modeling of fixed bed downdraft biomass gasification: Application on lab-scale and industrial reactors,” *Int. J. ENERGY Res.*, vol. 38, no. 4, pp. 319–338, 2014, doi: <https://doi.org/10.1002/er.3045>.
- [50] J. Watson, Y. Zhang, B. Si, W. T. Chen, and R. de Souza, “Gasification of biowaste: A critical review and outlooks,” *Renew. Sustain. Energy Rev.*, vol. 83, no. August 2017, pp. 1–17, 2018, doi: 10.1016/j.rser.2017.10.003.
- [51] P. Weerachanchai, M. Horio, and C. Tangsathitkulchai, “Effects of gasifying conditions and bed materials on fluidized bed steam gasification of wood biomass,” *Bioresour. Technol.*, vol. 100, no. 3, pp. 1419–1427, 2009, doi: 10.1016/j.biortech.2008.08.002.

- [52] L. Emami Taba, M. F. Irfan, W. A. M. Wan Daud, and M. H. Chakrabarti, “The effect of temperature on various parameters in coal, biomass and CO-gasification: A review,” *Renew. Sustain. Energy Rev.*, vol. 16, no. 8, pp. 5584–5596, 2012, doi: 10.1016/j.rser.2012.06.015.
- [53] P. Lahijani and Z. A. Zainal, “Gasification of palm empty fruit bunch in a bubbling fluidized bed: A performance and agglomeration study,” *Bioresour. Technol.*, vol. 102, no. 2, pp. 2068–2076, Jan. 2011, doi: 10.1016/J.BIORTECH.2010.09.101.
- [54] F. Pinto *et al.*, “Effect of experimental conditions on co-gasification of coal, biomass and plastics wastes with air/steam mixtures in a fluidized bed system,” *Fuel*, vol. 82, no. 15–17, pp. 1967–1976, Oct. 2003, doi: 10.1016/S0016-2361(03)00160-1.
- [55] L. Devi, K. J. Ptasiński, and F. J. J. G. Janssen, “A review of the primary measures for tar elimination in biomass gasification processes,” *Biomass and Bioenergy*, vol. 24, no. 2, pp. 125–140, 2003, doi: 10.1016/S0961-9534(02)00102-2.
- [56] U. Arena, “Fluidized bed gasification,” in *Fluidized Bed Technologies for Near-Zero Emission Combustion and Gasification*, F. Scala, Ed. Woodhead Publishing, 2013.
- [57] S. J. Park *et al.*, “Gasification operational characteristics of 20-tons-Per-Day rice husk fluidized-bed reactor,” *Renew. Energy*, vol. 169, pp. 788–798, 2021, doi: 10.1016/j.renene.2021.01.045.
- [58] M. L. Mastellone, L. Zaccariello, D. Santoro, and U. Arena, “The O<sub>2</sub>-enriched air gasification of coal, plastics and wood in a fluidized bed reactor,” *Waste Manag.*, vol. 32, no. 4, pp. 733–742, 2012, doi: 10.1016/j.wasman.2011.09.005.
- [59] D. Mallick, P. Mahanta, and V. S. Moholkar, “Co-gasification of biomass blends: Performance evaluation in circulating fluidized bed gasifier,” *Energy*, vol. 192, 2020, doi: 10.1016/j.energy.2019.116682.
- [60] Zhongqing Ma, J. Ye, C. Zhao, and Q. Zhang, “Gasification of Rice Husk in a Downdraft Gasifier: The Effect of Equivalence Ratio on the Gasification Performance, Properties, and Utilization Analysis of Byproducts of Char and Tar,” *BioResources*, vol. 10, no. 2, pp. 2888–2902, 2015, [Online]. Available: <https://ojs.cnr.ncsu.edu/index.php/BioRes/article/view/6859>.
- [61] S. W. Han *et al.*, “Gasification characteristics of waste plastics (SRF) in a bubbling fluidized bed: Effects of temperature and equivalence ratio,” *Energy*, vol. 238, p. 121944, Jan. 2022, doi: 10.1016/J.ENERGY.2021.121944.
- [62] D. Mallick, P. Mahanta, and V. S. Moholkar, “Co-gasification of coal and biomass blends: Chemistry and engineering,” *Fuel*, vol. 204, pp. 106–128, 2017, doi: 10.1016/j.fuel.2017.05.006.
- [63] M. L. Mastellone, L. Zaccariello, and U. Arena, “Co-gasification of coal, plastic waste and wood in a bubbling fluidized bed reactor,” *Fuel*, vol. 89, no. 10, pp. 2991–3000, 2010, doi: 10.1016/j.fuel.2010.05.019.
- [64] K. Kang, N. B. Klinghoffer, I. ElGhamrawy, and F. Berruti, “Thermochemical conversion of agroforestry biomass and solid waste using decentralized and mobile systems for

- renewable energy and products,” *Renew. Sustain. Energy Rev.*, vol. 149, no. October 2020, p. 111372, 2021, doi: 10.1016/j.rser.2021.111372.
- [65] G. Lopez, A. Erkiaga, M. Amutio, J. Bilbao, and M. Olazar, “Effect of polyethylene co-feeding in the steam gasification of biomass in a conical spouted bed reactor,” *Fuel*, vol. 153, no. x, pp. 393–401, 2015, doi: 10.1016/j.fuel.2015.03.006.
- [66] M. Inayat, S. A. Sulaiman, J. C. Kurnia, and M. Shahbaz, “Effect of various blended fuels on syngas quality and performance in catalytic co-gasification: A review,” *Renew. Sustain. Energy Rev.*, vol. 105, no. July 2018, pp. 252–267, 2019, doi: 10.1016/j.rser.2019.01.059.
- [67] F. Pinto, C. Franco, R. N. André, M. Miranda, I. Gulyurtlu, and I. Cabrita, “Co-gasification study of biomass mixed with plastic wastes,” *Fuel*, vol. 81, no. 3, pp. 291–297, 2002, doi: 10.1016/S0016-2361(01)00164-8.
- [68] P. Brachi, R. Chirone, F. Miccio, M. Miccio, A. Picarelli, and G. Ruoppolo, “Fluidized bed co-gasification of biomass and polymeric wastes for a flexible end-use of the syngas: Focus on bio-methanol,” *Fuel*, vol. 128, pp. 88–98, Jul. 2014, doi: 10.1016/J.FUEL.2014.02.070.
- [69] T. Robinson, B. Bronson, P. Gogolek, and P. Mehrani, “Comparison of the air-blown bubbling fluidized bed gasification of wood and wood – PET pellets,” *FUEL*, vol. 178, pp. 263–271, 2016, doi: 10.1016/j.fuel.2016.03.038.
- [70] M. M. Yu, M. S. Masnadi, J. R. Grace, X. T. Bi, C. J. Lim, and Y. Li, “Co-gasification of biosolids with biomass: Thermogravimetric analysis and pilot scale study in a bubbling fluidized bed reactor,” *Bioresour. Technol.*, vol. 175, pp. 51–58, Jan. 2015, doi: 10.1016/J.BIORTECH.2014.10.045.
- [71] S. Akkache, A. B. Hernández, G. Teixeira, F. Gelix, N. Roche, and J. H. Ferrasse, “Co-gasification of wastewater sludge and different feedstock: Feasibility study,” *Biomass and Bioenergy*, vol. 89, pp. 201–209, Jun. 2016, doi: 10.1016/J.BIOMBIOE.2016.03.003.
- [72] T. Robinson, B. Bronson, P. Gogolek, and P. Mehrani, “Air-Blown Bubbling Fluidized Bed Co-Gasification of Woody Biomass and Refuse Derived Fuel,” vol. 95, no. September 2016, pp. 55–61, 2017, doi: 10.1002/cjce.22641.
- [73] J. Dai, H. Cui, and J. R. Grace, “Biomass feeding for thermochemical reactors,” *Prog. Energy Combust. Sci.*, vol. 38, no. 5, pp. 716–736, Oct. 2012, doi: 10.1016/J.PECS.2012.04.002.
- [74] P. Brachi, R. Chirone, F. Miccio, M. Miccio, A. Picarelli, and G. Ruoppolo, “Fluidized bed co-gasification of biomass and polymeric wastes for a flexible end-use of the syngas : Focus on bio-methanol,” *FUEL*, vol. 128, pp. 88–98, 2014, doi: 10.1016/j.fuel.2014.02.070.
- [75] E. M. A. Edreis, X. Li, C. Xu, and H. Yao, “Kinetic study and synergistic interactions on catalytic CO<sub>2</sub> gasification of Sudanese lower sulphur petroleum coke and sugar cane bagasse,” *J. Mater. Res. Technol.*, vol. 6, no. 2, pp. 147–157, Apr. 2017, doi: 10.1016/J.JMRT.2016.09.001.
- [76] M. S. Masnadi *et al.*, “Fuel characterization and co-pyrolysis kinetics of biomass and fossil fuels,” *Fuel*, vol. 117, pp. 1204–1214, 2014, doi: 10.1016/j.fuel.2013.02.006.

- [77] V. Nemanova, A. Abedini, T. Liliedahl, and K. Engvall, “Co-gasification of petroleum coke and biomass,” *Fuel*, vol. 117, no. PART A, pp. 870–875, Jan. 2014, doi: 10.1016/J.FUEL.2013.09.050.
- [78] C. Cao, Y. He, G. Wang, H. Jin, and Z. Huo, “Co-gasification of Alkaline Black Liquor and Coal in Supercritical Water at High Temperatures (600–750 °C),” *Energy & Fuels*, vol. 31, no. 12, pp. 13585–13592, Dec. 2017, doi: 10.1021/acs.energyfuels.7b03044.
- [79] X. Zhan, Z. Zhou, W. Kang, and F. Wang, “Promoted slurryability of petroleum coke–water slurry by using black liquor as an additive,” *Fuel Process. Technol.*, vol. 91, no. 10, pp. 1256–1260, Oct. 2010, doi: 10.1016/J.FUPROC.2010.04.006.
- [80] P. Lahijani, Z. A. Zainal, A. R. Mohamed, and M. Mohammadi, “Co-gasification of tire and biomass for enhancement of tire-char reactivity in CO<sub>2</sub> gasification process,” *Bioresour. Technol.*, vol. 138, pp. 124–130, Jun. 2013, doi: 10.1016/J.BIORTECH.2013.03.179.
- [81] F. Miccio, F. Raganati, P. Ammendola, F. Okasha, and M. Miccio, “Fluidized Bed Combustion and Gasification of Fossil and Renewable Slurry Fuels,” 2021, doi: 10.3390/en14227766.
- [82] G. Jiménez-García, R. Aguilar-López, and R. Maya-Yescas, “The fluidized-bed catalytic cracking unit building its future environment,” *Fuel*, vol. 90, no. 12, pp. 3531–3541, Dec. 2011, doi: 10.1016/J.FUEL.2011.03.045.
- [83] H. S. Kwon, J. H. Moon, U. Do Lee, J. J. Yoon, G. P. van Walsum, and B. H. Um, “Fractionation and gasification of black liquor derived from kraft pulping,” *J. Ind. Eng. Chem.*, vol. 34, pp. 122–129, Feb. 2016, doi: 10.1016/J.JIEC.2015.10.044.
- [84] D. Geldart, *Gas Fluidization Technology*. John Wiley, 1986.
- [85] C. E. Agu, L. A. Tokheim, M. Eikeland, and B. M. E. Moldestad, “Determination of onset of bubbling and slugging in a fluidized bed using a dual-plane electrical capacitance tomography system,” *Chem. Eng. J.*, vol. 328, pp. 997–1008, 2017, doi: 10.1016/j.cej.2017.07.098.
- [86] R. J. Evans and T. A. Milne, “Chemistry of Tar Formation and Maturation in the Thermochemical Conversion of Biomass,” *Dev. Thermochem. Biomass Convers.*, no. November, pp. 803–816, 1997, doi: 10.1007/978-94-009-1559-6\_64.
- [87] W. Zhang *et al.*, “Gas cleaning strategies for biomass gasification product gas,” *Int. J. Low-Carbon Technol.*, vol. 7, no. 2, pp. 69–74, 2012, doi: 10.1093/ijlct/ctr046.
- [88] T. Bui, R. Loof, and S. . Bhattacharya, “Multi-stage reactor for thermal gasification of wood,” *Energy*, vol. 19, no. 4, pp. 397–404, 1994.
- [89] M. L. Valderrama Rios, A. M. González, E. E. S. Lora, and O. A. Almazán del Olmo, “Reduction of tar generated during biomass gasification: A review,” *Biomass and Bioenergy*, vol. 108, no. July 2017, pp. 345–370, 2018, doi: 10.1016/j.biombioe.2017.12.002.
- [90] R. Mohtadi, W. -k. Lee, S. Cowan, J. W. Van Zeeand, and M. Murthy, “Effects of Hydrogen

- Sulfide on the Performance of a PEMFC,” *Electrochem. Solid-State Lett.*, vol. 6, no. 12, p. 272, 2003, [Online]. Available: <https://iopscience.iop.org/article/10.1149/1.1621831/pdf>.
- [91] W. Torres, S. S. Pansare, and J. G. Goodwin, “Hot gas removal of tars, ammonia, and hydrogen sulfide from biomass gasification gas,” *Catal. Rev. - Sci. Eng.*, vol. 49, no. 4, pp. 407–456, 2007, doi: 10.1080/01614940701375134.
- [92] Y. Shen, P. Zhao, Q. Shao, D. Ma, F. Takahashi, and K. Yoshikawa, “In-situ catalytic conversion of tar using rice husk char-supported nickel-iron catalysts for biomass pyrolysis/gasification,” *Appl. Catal. B Environ.*, vol. 152–153, no. 1, pp. 140–151, 2014, doi: 10.1016/j.apcatb.2014.01.032.
- [93] L. Devi, K. J. Ptasinski, F. J. J. G. Janssen, S. V. B. Van Paasen, P. C. A. Bergman, and J. H. A. Kiel, “Catalytic decomposition of biomass tars: Use of dolomite and untreated olivine,” *Renew. Energy*, vol. 30, no. 4, pp. 565–587, 2005, doi: 10.1016/j.renene.2004.07.014.
- [94] S. You and X. Wang, *On the carbon abatement potential and economic viability of biochar production systems: Cost-benefit and life cycle assessment*. Elsevier Inc., 2018.
- [95] Y. Chai, N. Gao, M. Wang, and C. Wu, “H<sub>2</sub> production from co-pyrolysis/gasification of waste plastics and biomass under novel catalyst Ni-CaO-C,” *Chem. Eng. J.*, vol. 382, no. July 2019, p. 122947, 2020, doi: 10.1016/j.cej.2019.122947.
- [96] D. Serrano, M. Kwapinska, A. Horvat, S. Sánchez-Delgado, and J. J. Leahy, “*Cynara cardunculus* L. gasification in a bubbling fluidized bed: The effect of magnesite and olivine on product gas, tar and gasification performance,” *Fuel*, vol. 173, pp. 247–259, Jun. 2016, doi: 10.1016/J.FUEL.2016.01.051.
- [97] C. Christodoulou, D. Grimekis, K. D. Panopoulos, E. P. Pachatouridou, E. F. Iliopoulou, and E. Kakaras, “Comparing calcined and un-treated olivine as bed materials for tar reduction in fluidized bed gasification,” *Fuel Process. Technol.*, vol. 124, pp. 275–285, 2014, doi: 10.1016/j.fuproc.2014.03.012.
- [98] E. Karimi *et al.*, “Red Mud as a Catalyst for the Upgrading of Hemp-Seed Pyrolysis Bio-oil,” *Energy & Fuels*, vol. 24, no. 12, pp. 6586–6600, Nov. 2010, doi: 10.1021/ef101154d.
- [99] L. Cheng *et al.*, “Tar elimination from biomass gasification syngas with bauxite residue derived catalysts and gasification char,” *Appl. Energy*, vol. 258, p. 114088, Jan. 2020, doi: 10.1016/J.APENERGY.2019.114088.
- [100] A. Scientific Thermo, “FlashSmart™ Elemental Analyzer,” 2021. <https://www.thermofisher.com/order/catalog/product/11206100> (accessed Dec. 22, 2021).
- [101] C. Christodoulou, D. Grimekis, K. D. Panopoulos, E. P. Pachatouridou, E. F. Iliopoulou, and E. Kakaras, “Comparing calcined and un-treated olivine as bed materials for tar reduction in fluidized bed gasification,” *Fuel Process. Technol.*, vol. 124, pp. 275–285, Aug. 2014, doi: 10.1016/J.FUPROC.2014.03.012.
- [102] W. Tauqir, M. Zubair, and H. Nazir, “Parametric analysis of a steady state equilibrium-

- based biomass gasification model for syngas and biochar production and heat generation,” *Energy Convers. Manag.*, vol. 199, no. August, p. 111954, 2019, doi: 10.1016/j.enconman.2019.111954.
- [103] Y. Furusawa, H. Taguchi, S. N. Ismail, S. Thangavel, K. Matsuoka, and C. Fushimi, “Estimation of cold gas efficiency and reactor size of low-temperature gasifier for advanced-integrated coal gasification combined cycle systems,” *Fuel Process. Technol.*, vol. 193, pp. 304–316, Oct. 2019, doi: 10.1016/J.FUPROC.2019.05.023.
- [104] Y. D. Kim *et al.*, “Air-blown gasification of woody biomass in a bubbling fluidized bed gasifier,” *Appl. Energy*, vol. 112, pp. 414–420, 2013, doi: 10.1016/j.apenergy.2013.03.072.
- [105] L. Zaccariello and M. L. Mastellone, “Fluidized-bed gasification of plastic waste, wood, and their blends with coal,” *Energies*, vol. 8, no. 8, pp. 8052–8068, 2015, doi: 10.3390/en8088052.
- [106] J. J. R. Behainne and J. D. Martinez, “Performance analysis of an air-blown pilot fluidized bed gasifier for rice husk,” *Energy Sustain. Dev.*, vol. 18, no. 1, pp. 75–82, Feb. 2014, doi: 10.1016/J.ESD.2013.11.008.
- [107] J. P. Makwana, A. K. Joshi, G. Athawale, D. Singh, and P. Mohanty, “Air gasification of rice husk in bubbling fluidized bed reactor with bed heating by conventional charcoal,” *Bioresour. Technol.*, vol. 178, pp. 45–52, Feb. 2015, doi: 10.1016/J.BIORTECH.2014.09.111.
- [108] M. P. Aznar, M. A. Caballero, J. A. Sancho, and E. Francés, “Plastic waste elimination by co-gasification with coal and biomass in fluidized bed with air in pilot plant,” *Fuel Process. Technol.*, vol. 87, no. 5, pp. 409–420, May 2006, doi: 10.1016/J.FUPROC.2005.09.006.
- [109] Ian Narvaez, Alberto Oriio, Maria P. Aznar, and Jose Corella, “Biomass Gasification with Air in an Atmospheric Bubbling Fluidized Bed . Effect of Six Operational Variables on the Quality of,” vol. 5885, no. 95, pp. 2110–2120, 1996, doi: 10.1021/ie9507540.
- [110] H. L. Zhu *et al.*, “Co-gasification of beech-wood and polyethylene in a fluidized-bed reactor,” *Fuel Process. Technol.*, vol. 190, no. February, pp. 29–37, 2019, doi: 10.1016/j.fuproc.2019.03.010.
- [111] M. L. Mastellone and L. Zaccariello, “Metals flow analysis applied to the hydrogen production by catalytic gasification of plastics,” *Int. J. Hydrogen Energy*, vol. 38, no. 9, pp. 3621–3629, Mar. 2013, doi: 10.1016/J.IJHYDENE.2012.12.111.
- [112] S. Rapagna, A. D’orazio, K. Gallucci, P. U. Foscolo, M. Nacken, and S. Heidenreich, “Hydrogen rich gas from catalytic steam gasification of biomass in a fluidized bed containing catalytic filters,” *Chem. Eng. Trans.*, vol. 37, no. November, pp. 157–162, 2014, doi: 10.3303/CET1437027.
- [113] C. Gai and Y. Dong, “Experimental study on non-woody biomass gasification in a downdraft gasifier,” *Int. J. Hydrogen Energy*, vol. 37, no. 6, pp. 4935–4944, 2012, doi: 10.1016/j.ijhydene.2011.12.031.
- [114] H. Nam, D. A. Rodriguez-Alejandro, S. Adhikari, C. Brodbeck, S. Taylor, and J. Johnson,

- “Experimental investigation of hardwood air gasification in a pilot scale bubbling fluidized bed reactor and CFD simulation of jet/grid and pressure conditions,” *Energy Convers. Manag.*, vol. 168, pp. 599–610, Jul. 2018, doi: 10.1016/J.ENCONMAN.2018.05.003.
- [115] U. Arena and F. Di Gregorio, “Energy generation by air gasification of two industrial plastic wastes in a pilot scale fluidized bed reactor,” *Energy*, vol. 68, pp. 735–743, Apr. 2014, doi: 10.1016/J.ENERGY.2014.01.084.
- [116] F. J. Mastral, E. Esperanza, C. Berruenco, M. Juste, and J. Ceamanos, “Fluidized bed thermal degradation products of HDPE in an inert atmosphere and in air–nitrogen mixtures,” *J. Anal. Appl. Pyrolysis*, vol. 70, no. 1, pp. 1–17, Oct. 2003, doi: 10.1016/S0165-2370(02)00068-2.
- [117] E. R. Widjaya, G. Chen, L. Bowtell, and C. Hills, “Gasification of non-woody biomass: A literature review,” *Renew. Sustain. Energy Rev.*, vol. 89, no. March, pp. 184–193, 2018, doi: 10.1016/j.rser.2018.03.023.
- [118] P. Sahoo and A. Sahoo, “Hydrodynamic studies on fluidization of Red mud: CFD simulation,” *Adv. Powder Technol.*, vol. 25, no. 6, pp. 1699–1708, 2014, doi: 10.1016/j.appt.2014.06.017.
- [119] M. Wang and X. Liu, “Applications of red mud as an environmental remediation material: A review,” *J. Hazard. Mater.*, vol. 408, no. July 2020, p. 124420, 2021, doi: 10.1016/j.jhazmat.2020.124420.
- [120] J. Kim, T. Mun, J. Kim, and J. Kim, “Air gasification of mixed plastic wastes using a two-stage gasifier for the production of producer gas with low tar and a high caloric value,” *Fuel*, vol. 90, no. 6, pp. 2266–2272, 2011, doi: 10.1016/j.fuel.2011.02.021.
- [121] S. Osipovs, “Comparison of efficiency of two methods for tar sampling in the syngas,” *Fuel*, vol. 103, pp. 387–392, Jan. 2013, doi: 10.1016/J.FUEL.2012.05.021.

## 5. Appendices

### Appendix A. Equipment modification

The reactor was previously used to assess the agglomeration of bed material that leads to de-fluidization phenomena. so the system wasn't utilizing all the components as would do a gasification system. For this study, some of these issues were addressed to better utilize the whole system for the gasification.

The feeding system consists of a hopper, a screw feeder, a rotary valve, a vibrator, and piping. The piping has been stuck so the feedstock restricted from entering the reactor due to the melting of the residue that contains plastics from the previous run (Figure 5-1). When the run started the new material got stuck at the elbow by the sticky old molten material and the vibrator did not effective with non flowable matter. As a solution, a ½" hole was introduced to allows the operator to flush the elbow after the experiment is done. It can also be used as inert gas inlet to prevent backflow of the produced gas if it caused any challenges for the feeding system.

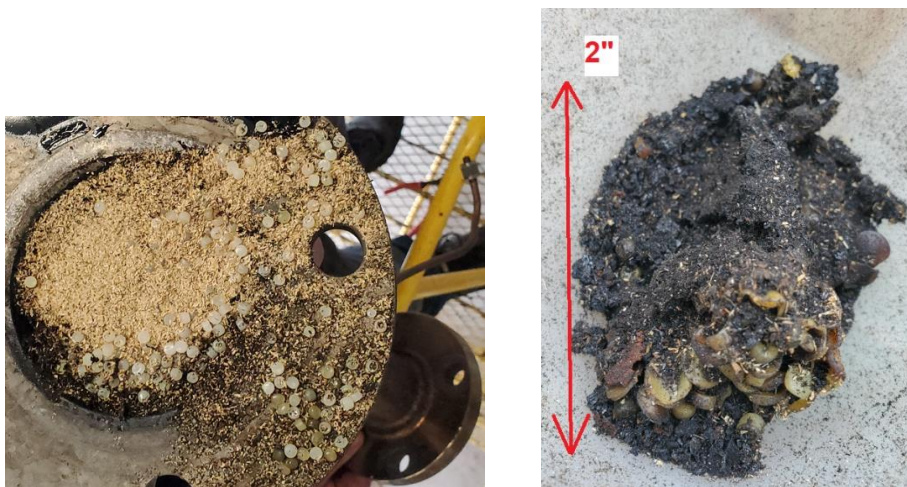


**Figure 5-1 Blockage of feeding line caused by materials residue.**



**Figure 5-2 New manufactured inlet to blow any residue after the experiment, or continuously supply inert gas (N<sub>2</sub>)**

Before starting the experiments, the feeding system was not sealed at the hopper which was leading to the escape of the product gas and the contamination of the feedstock with tar, this can lead to the formation of sticky tar within the feedstock that acts as a cohesive material and affect the flowability of the feedstock. At extreme case, it can cause shut down of operation as mentioned previously. It has been decided to seal the hopper cover and consider the feed system as batch instead of continuous feeding, however, if it is needed to be continuous, another sealed container can be mounted on the top of the current hopper and use two valves to continuously feed the hopper without compromising the system's integrity.



Figure 5-3 a- un-sealed hopper b- sealed hopper cap and mounted with valve

## **Appendix B. Tar accumulation downstream the reactor**

The product gases exit the top of the reactor to a 1” piping that ends at the cyclone. Due to the drop of the temperature at this area, the condensable hydrocarbon (tar) got the opportunity to accumulate at this line and cause plugging, consequently shut the operation down. The challenge of tar needs to be addressed by controlling the temperature downstream the reactor to prevent the tar condensation. It also needs a standard tar sampling system for further study. There are two techniques for tar collection; solid-phase adsorption (SPA) for quantitative analysis and cold solvent trapping (CST) for qualitative analysis [121].



**Figure 5-4 Tar accumulated in the reactor-cyclone connection**

## **Appendix C. Air Preheater performance**

The air, that was being pre-heated before entering the reactor, temperature was around 300 °C. The performance of the heating was examined at different air flowrates. The heat transfer was enhanced by increasing the transfer surface area using steel beads. It was noticed that, the heat transfer increases as the air speed (Reynold number) increases inside the pipe (higher flow rate) due to the higher heat transfer coefficient, this effect can be understood from the equation

$$h = \frac{0.027 k (Re)^{0.8} Pr^{1/3}}{d} \left( \frac{\mu}{\mu_w} \right)^{0.14}$$

where  $h$ ,  $k$ ,  $Re$ ,  $Pr$ ,  $d$ ,  $\mu$ , and  $\mu_w$  are the heat transfer coefficient, conductivity of tube, Reynold and Prandtl numbers, diameter of the tube, viscosity of the fluid at bulk and wall temperatures, respectively.

The below table shows the values of the exit temperature of air at different flow rates.

Air rate (scfh)	Air post preheater (°C)
10	520
15	531
25	660

## Appendix D. Feeding calibration

The screw feeding system is consists of twin screws (Figure 5-5) that are coupled to a gearbox which has variable speed, which can be controlled by the K-tron module (Figure 2-3). The mechanism of the variable speed is based on the available volume between the screws, therefore it cannot relate to the mass of the feedstock. The desired mass flow rate of the feedstock needs to be calibrated for each size (density) by measuring the actual throughput of the system for each speed. Calibration curves are mentioned below as examples for the rice husk.



**Figure 5-5 Screw feeder (uncovered)**

Set point/time (min)	2	4	6	8	10	12	average
1	28.1	29.8	29	30.3	25.6	26.9	28.5
1.2	35.5	36.5	35.8	34.1	32.5	29.3	34.8
2	57	55.5	53.7	55.1			55.3

**Figure 5-6 Feeding system module throughput at different set points**

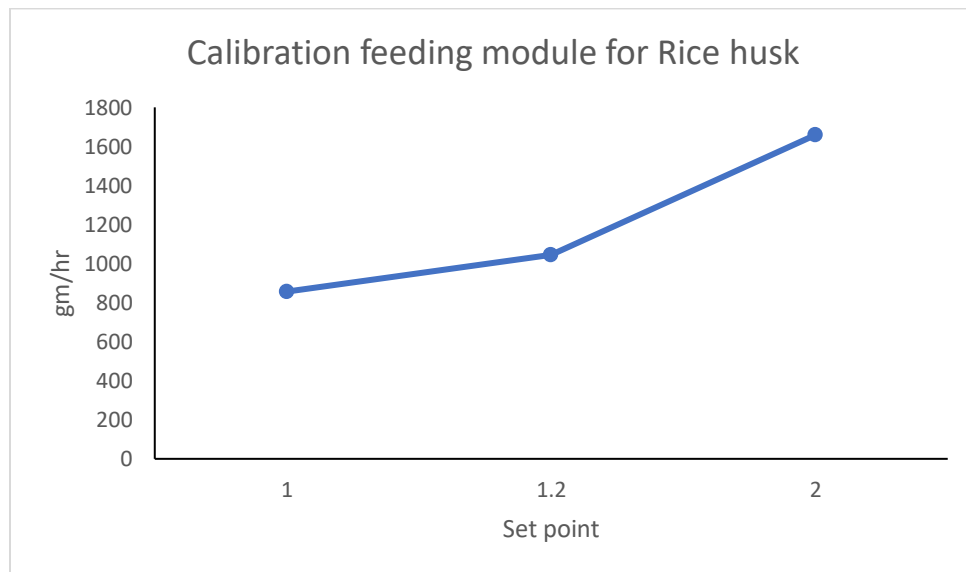


**Figure 5-7 Calibration the feeding module for Rice husk**

### Appendix E. Order and compositions of feedstock used in different runs

Run number	Run date	Feedstock	Bed material
1	14-May	Birch saw dust	sand
2	20-May	Birch saw dust	sand
3	24-Jun	Birch saw dust	Olivine
4	7-Jul	Birch SD +15% LDPE	Sand
5	8-Jul	Birch SD +30% LDPE	Sand
6	13-Jul	Birch SD +50% LDPE	Sand
7	19-Jul	Birch SD +50% LDPE	Olivine
8	22-Jul	Birch SD +50% HDPE	Olivine
9	29-Jul	Birch SD +50% HDPE	sand
10	16-Aug	Birch SD +50% HDPE	Olivine
11	18-Aug	Birch SD +50% HDPE	sand
12	27-Aug	Birch SD +50% LDPE	Olivine
13	30-Aug	Birch SD +50% HDPE	Olivine
14	1-Sep	Birch SD +50% HDPE	sand
15	8-Sep	Birch SD +50% LDPE	sand
16	14-Sep	Birch SD +50% LDPE	Olivine
17	22-Sep	Rice Husk +50% LDPE	Olivine
18	23-Sep	Rice Husk +50% LDPE	sand
19	27-Sep	Rice Husk +50% HDPE	Olivine
20	27-Oct	Rice Husk +50% HDPE	Olivine
21	28-Oct	Rice Husk +50% HDPE	sand
22	3-Nov	Rice Husk +50% LDPE	Olivine
23	8-Nov	Rice Husk +50% LDPE	sand
24	23-Nov	Birch SD +50% LDPE	Red mud
25	24-Nov	Birch SD +50% HDPE	Red mud
26	29-Nov	Rice Husk +50% LDPE	Red mud
27	6-Dec	Rice Husk +50% HDPE	Red mud
28	9-Dec	Rice Husk	sand
29	9-Dec	Rice Husk	sand
30	9-Dec	Rice Husk	sand
31	24-Jan	Birch SD +50% LDPE	sand
32	24-Jan	Birch SD +50% LDPE	sand
33	24-Jan	Birch SD +50% LDPE	sand

## **Appendix F. Permission for the Table 1-3 and the Figure 1-4**

This Agreement between UWO -- Islam ElGhamrawy ("You") and Elsevier ("Elsevier") consists of your license details and the terms and conditions provided by Elsevier and Copyright Clearance Center.

License Number	5254241282090
License date	Feb 22, 2022
Licensed Content Publisher	Elsevier
Licensed Content Publication	Renewable and Sustainable Energy Reviews
Licensed Content Title	Effect of various blended fuels on syngas quality and performance in catalytic co-gasification: A review
Licensed Content Author	Muddasser Inayat,Shaharin A. Sulaiman,Jundika Candra Kurnia,Muhammad Shahbaz
Licensed Content Date	May 1, 2019
Licensed Content Volume	105
Licensed Content Issue	n/a
Licensed Content Pages	16

This Agreement between UWO -- Islam ElGhamrawy ("You") and Elsevier ("Elsevier") consists of your license details and the terms and conditions provided by Elsevier and Copyright Clearance Center.

License Number	5275420029454
License date	Mar 24, 2022
Licensed Content Publisher	Elsevier
Licensed Content Publication	Elsevier Books
Licensed Content Title	Fluidized Bed Technologies for Near-Zero Emission Combustion and Gasification
Licensed Content Author	U. Arena
Licensed Content Date	Jan 1, 2013
Licensed Content Pages	48
Start Page	765
End Page	812
Type of Use	reuse in a thesis/dissertation
Portion	figures/tables/illustrations